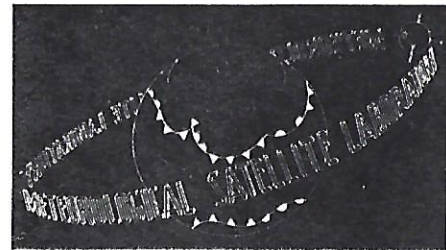


U. S DEPARTMENT OF COMMERCE
ENVIRONMENTAL SCIENCE SERVICES ADMINISTRATION

QC
879.5
.U45
no.37

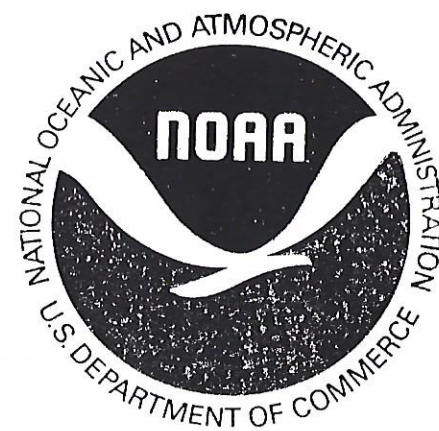


METEOROLOGICAL SATELLITE LABORATORY
REPORT NO 37

Mesoscale Cellular Convection

WASHINGTON, D. C.
MAY 1966

INTERLIBRARY LOAN
from



NOAA Central Library
Silver Spring, MD
Date due: 11/7/97
(unless recalled earlier)

ILL: 19304440

You can request renewals
on OCLC (OCLC code: OLA)
or call (301) 713-2600 x113
and ask for Interlibrary Loan.

*Please return material to:

NOAA Central Library, E/OC4
Interlibrary Loan
1315 East-West Highway
SSMC3, 2nd Floor
Silver Spring, MD 20910

IT IS A PLEASURE TO SERVE YOU!

METEOROLOGICAL SATELLITE LABORATORY REPORTS

(1-3, 5-23, 36, 28-33 are available through the Clearinghouse for Federal Scientific and Technical Information, U. S. Department of Commerce, Sills Building, Port Royal Road, Springfield, Virginia 22151. The CFSTI number and price follow each entry.)

- Number
 1. Cloud Conference Summary, L. F. Whitney, Jr., (July 1960)
 PB 163727 \$2.60
 *2. Analysis of Project Hugo Test Firing, December 5, 1958, L. F. Hubert, (August 1960) PB 163728 \$5.60
 *3. Preliminary Studies of Atmospheric Energy Parameters, J. S. Winston, (January 1961) PB 163729 \$3.60
 4. Open
 5. TIROS I - Camera Attitude Data, Analysis of Location Errors, and Derivation of Correction for Calibration, L. F. Hubert, (April 1961) N 6211116 \$6.60
Supplement to 5: Canadian Grids for TIROS I, Additional Orientation Data, Errata, L. F. Hubert, (June 1961) N 6211117 \$4.60
 *6. Nimbus Data Utilization Plan, (Anon), (April 1961) PB 163732 \$2.60
 7. Identification of Cloud Forms from TIROS I Pictures, C. O. Erickson and L. F. Hubert, (June 1961) N 6214286 \$7.60
 8. Ice Photography from the Meteorological Satellites TIROS I and TIROS II, D. Q. Wark and R. W. Popham, (March 1962) PB 163734 \$4.60
 *9. Documentation for TIROS III Television Data, L. F. Hubert, (March 1962) PB 163735 \$6.60
 10. Infrared Flux and Surface Temperature Determinations from TIROS Radiometer Measurements, D. Q. Wark, G. Yamamoto, and J. H. Lienesch, (August 1962) N 6311881 \$8.60
Supplement to 10: (April 1963) PB 165208 \$1.10
 11. Perspective Locator Grids for TIROS Pictures, M. H. Frankel and C. L. Bristol, (October 1962) PB 163737 \$4.60
 12. Catalog of Supplemental Meteorological Data Concurrent with TIROS Satellite Observations (TIROS I-V), R. L. Pyle, (August 1962) PB 163738 \$4.60
 *13. Conference on Sferics Measurements, S. Soules (Ed.), (October 1962) PB 163739 \$5.60
 14. A Technique for Precise Analysis for Satellite Data - Vol. 1, Photogrammetry, T. Fujita, (February 1963) PB 163740 \$9.60
 15. Calibration of Image Distortion in TIROS Wide Angle Photography, R. C. Doolittle, (July 1963) PB 163741 \$5.60
 16. Documentation for TIROS IV Television Data, R. L. Pyle, (May 1963) PB 163742 \$8.10
 17. On the Use of Redundancy in the Design of Operational Satellites, S. F. Singer, (April 1963) PB 163743 \$1.60
 18. An Analysis of CDA Station Effectiveness in Relation to Satellite Orbit, R. L. Pyle and S. F. Singer, (July 1963) PB 163744 \$3.60

(Continued on inside of back cover)

* Out of Print

This paper has been printed as a manuscript report for the information of selected interested organizations. As this reproduction does not constitute formal scientific publication, any reference to it in published articles and scientific literature should identify it as a manuscript of the Environmental Science Services Administration, National Environmental Satellite Center.

U. S. DEPARTMENT OF COMMERCE

John T. Connor, Secretary

ENVIRONMENTAL SCIENCE SERVICES ADMINISTRATION

Robert M. White, Administrator

U. S. National Environmental Satellite Center,

METEOROLOGICAL SATELLITE LABORATORY

REPORT NO. 37

MESOSCALE CELLULAR CONVECTION

by

Lester F. Hubert

Washington, D. C.
May 1966

LIBRARY

N.O.A.A.
U.S. Dept. of Commerce

QC
879.5
045
mo.-7

136 851

TABLE OF CONTENTS

	Page
	iv
LIST OF FIGURES	iv
LIST OF TABLES	vi
ABSTRACT	1
I. INTRODUCTION	1
II. DOCUMENTATION OF CELLS	2
Picture interpretation and measurement.....	6
Satellite pictures and associated data.....	7
III. A HYPOTHESIS AND ITS THEORETICAL AND EXPERIMENTAL BACKGROUND	30
Direction of Circulation	30
Initial Instability, shear, cell size, and rotation	49
IV. SUGGESTIONS FOR FUTURE WORK.....	60
V. SUMMARY OF CELL CHARACTERISTICS AND CONCLUSIONS.....	63
ACKNOWLEDGEMENTS	65
REFERENCES	66

U.S. National Environmental Satellite Center.	
Meteorological Satellite Laboratory report no.37. Mesoscale cellular convection, by Lester F. Hubert.	
136851 M07.362/2	
DATE	ISSUED TO USGS/NOAA
08/11/68	no. 37
SEP 24 1968	136851-3. October. Gens
10/11/68	4905 Duffield Rd., Suite 200, Fort
1/15/69	Seattle Center, Seattle, Wash.

136 851

LIST OF FIGURES

	Page
Figure 1. Gemini 5 picture of open cells and theoretical vertical motions.....	4
Figure 2. Gemini 6 picture of open cells.....	5
Figure 3. Gemini 6 picture of closed cells.....	5
Figure 4. Schematic cross section of open and closed cells...	7
Figure 5. Open cells in North Pacific January 11, 1964.....	8
Figure 6. Surface map and radiosonde 00 GMT January 11, 1964.	9
Figure 7. Open cells in North Pacific April 23, 1962.....	10
Figure 8. Surface map for 18 GMT April 23, 1962 and two radiosondes.....	11
Figure 9. Open cells in North Pacific November 19, 1963.....	12
Figure 10. Surface map for 18 GMT November 19, 1963.....	13
Figure 11. Open cells in North Atlantic September 19, 1962....	14
Figure 12. Surface map and radiosondes for 12 GMT September 16, 1962.....	15
Figure 13. Closed cells in subtropical North Pacific July 1, 1963.....	16
Figure 14. Surface map for 18 GMT July 1, 1963.....	17
Figure 15. Open and closed cells in North Pacific April 18, 1962.....	18
Figure 16. Surface map and radiosondes for 00 GMT April 19, 1962.....	19
Figure 17. Open and closed cells in North Pacific June 5, 1962	20
Figure 18. Surface map for 18 GMT June 5, 1962 and radiosonde for 00 GMT June 6, 1962.....	21
Figure 19. Open and closed cells in North Pacific April 16, 1963.....	22

LIST OF FIGURES (CONTINUED)

	Page
Figure 20. Surface map and radiosondes for 00 GMT April 17, 1963.....	23
Figure 21. Open and closed cells in the North Pacific April 17, 1963.....	24
Figure 22. Surface map for 18 GMT April 17, 1963 and radiosonde for 00 GMT April 18, 1963.....	25
Figure 23. Open and closed cells in the North Pacific April 25, 1963.....	26
Figure 24. Surface map for 18 GMT April 25, 1963 and radiosonde for 00 GMT April 26, 1963.....	27
Figure 25. Open cells and mixed pattern in North Pacific May 12, 1964.....	28
Figure 26. Surface map for 18 GMT May 12, 1964 and radiosonde for 00 GMT May 13, 1964.....	29
Figure 27. Hypothetical sounding and longwave net radiation...	38
Figure 28. Nimbus HRIR and TIROS VIII pictures of same area, day and night September 10, 1964.....	46
Figure 29. Nimbus HRIR and AVCS pictures of same area, day and night September 10, 1964.....	47
Figure 30. Nimbus AVCS picture of both cell types and a possible transitional form.....	48
Figure 31. Lines of cumuli in shallow cold air over Gulf of Mexico January 30, 1966 with surface map and radiosondes.....	51
Figure 32. Lines of cumuli in shallow cold air over western Atlantic January 31, 1966 with surface map and radiosondes.....	52
Figure 33. Cell diameter versus inversion height.....	54
Figure 34. Diameter:depth ratio versus angular speed and versus depth.....	59

MESOSCALE CELLULAR CONVECTION

ABSTRACT

The large areal extent of mesoscale cellular patterns in cumuli suggests there exists a scale of mesoscale convection that is significant to air-sea exchange mechanisms. The purpose here is to bring together a representative sample of satellite and associated meteorological data concerning these cells, and to propose a hypothesis for them that is based on the extant work on Bénard convection.

LIST OF TABLES	Page
TABLE 1. Longwave flux divergence and cooling rates for cloud and subcloud layers.....	38
TABLE 2. Summary of destabilizing temperature changes....	40
TABLE 3. Frequency of $V(T_s - T_a)$ [kt. $^{-\circ}$ C] by cell type....	43
TABLE 4. Data for plot of D/h vs Ω and h	58

As in the laboratory two classes of cells appear to exist: those with ascent in the cell centers and those with descent in the cell centers. Experiment and theory indicate this may be due to the vertical variation of eddy viscosity. It is suggested that the destabilizing effect of surface heating and cloud top cooling by radiation determine this vertical variation, and that these usually are of greater magnitude than evaporation cooling or release of latent heat. Shear and non-steady-state heating are unfavorable for these mesoscale cells, but rotation probably has no effect.

Suggestions for future work are to construct a theoretical model that incorporates anisotropic, variable, eddy exchanges and diabatic energy sources other than latent instability.

Suggested experimental work should be carried out in the atmosphere, not in the laboratory, and it should include measurements of eddy flux of heat and momentum as well as the diabatic energy sources.

I. INTRODUCTION

Meteorological satellites have shown a surprisingly high degree of mesoscale organization of convective cloudiness. The existence of such organization was previously known, but the degree and extent of this organization is a new observation. This scale of atmospheric motion is important because, occurring over very large areas of the ocean, it probably is a significant link in the interaction between the sea and the atmosphere.

When air is heated by a warmer water surface to produce the familiar convective clouds, the satellite data show that their distribution is not random, but rather that there is a strong tendency for the convective clouds to arrange themselves into patterns of convective cells on the scale of a few tens of miles in diameter.

Both experimental work and theory provide suggestive evidence that these cellular patterns are the result of preferred scales and configuration of the energy exchange mechanism. If this proves to be true then the flux of momentum, sensible heat, and water vapor are significantly affected by a convective circulation which has a characteristic horizontal scale of tens of miles as well as by the individual clouds that are one or two orders of magnitude smaller. A recent report by Zipser and LaSeur [33] shows that mesoscale organization is a significant tropical phenomenon. Earlier, Malkus [15], discussing variations within the trade wind layer, pointed out that one should enquire about "....slight inhomogeneities....on a 10 to 30 km. scale." The present writer suggests therefore that these meso-scale convective cells must be "calibrated" and accounted for in air-sea energy bookkeeping. It is therefore constructive to bring to general attention the empirical results derived from satellite data, and to point out their possible implications, even though these are speculative and tentative.

The purpose of this paper is to present empirical evidence of the mesoscale circulation and to suggest a hypothesis explaining this scale of convection. The hypothesis is based on the strong similarity of (inferred) atmospheric phenomena to small-scale phenomena produced experimentally. It is suggested that these mechanisms are analogous if (and only if) proper consideration is given to the differences between molecular and eddy exchange processes. If the proposed analogy is proper, the existing body of theoretical work on convection would yield insight into mesoscale organization in the atmosphere.

In the next section several typical examples are presented; it is followed by a section that presents the hypothesis and reviews the experimental and theoretical work on convection that has suggested the hypothesis. The review is not exhaustive, but rather includes only those items believed to be relevant to this hypothesis. Section IV presents some suggestions for experimental and theoretical research.

II. DOCUMENTATION OF CELLS*

Satellite data presented in this section suggest that mesoscale cellular patterns develop when convective cloudiness is maintained over a uniform surface for periods of the order of hours. Every outbreak of cold continental air over a warmer ocean contains such cells, presumably as soon as the water trajectory is sufficiently

* In this report the terms "cells" and "cellular convection" in the atmosphere will be used to mean conglomerates of cloud elements that are organized into cells with diameters of some tens of miles. "Cell" does not refer to the individual cumulus element even though the latter are also small scale cells.

long to develop an adequately thick layer and to permit the heat flux to achieve a quasi-steady-state.* Certain portions of oceanic anticyclones are also favored regions for the occurrence of cells. Consequently millions of square miles of the ocean surface are covered at all times with mesoscale cellular convection in various stages of development.

The cold air cells commonly are comprised of cumulus congestus and swelling cumuli, but some poorly formed cells are sometimes found in cumulonimbus cloud fields. Cells in the oceanic anticyclones are more commonly made up of trade wind cumuli and stratocumulus.

Two types of cellular organization occur, the "open cell" and the "closed cell." "Open cells" (figs. 1 and 2) are characterized by approximately polygonal clear areas surrounded by cloud walls. "Closed cells" (fig. 3) are approximately polygonal, cloud-covered areas surrounded by walls of clear air. As might be expected, many combinations and configurations have been observed. It is sometimes difficult to characterize a given pattern either as "open" or "closed" because the cell walls broaden or are interrupted.

Several examples of both cell types are included here. Most of the cases have been selected because there were ship observations within the cloud field at the nearest synoptic time. Figures 1, 2, and 3 are exceptions; no ship observations are shown, but the patterns are so well-photographed from manned spacecraft that they provide an excellent introduction to the subject.

The outstanding characteristic of the cells near the Cuban coast in figure 1 is the close approximation to the classical hexagonal shape. These open cells would be undetected by the standard satellite (television) pictures because the clouds walls are too thin and the cell diameter is very small. The median diameter of TIROS-observed cells is approximately 50 km., whereas these range from 5 to 10 km. A curious feature in figure 1 is the enhanced clouds at some of the hexagon corners. Compare the theoretical vertical motion field derived by Pellew & Southwell [20]. For that computation the authors considered the circulation to be upward in the cell center but presumably the same relative maxima at the cell corners would exist if the sign of ω were reversed.

Figure 2 shows open cells in which the cell wall clouds are somewhat more uniformly developed, but the cell shape is irregular. An interesting change of cell diameter is seen between the left and right sides of the field.

* This point is discussed in a later section under "Initial instability."

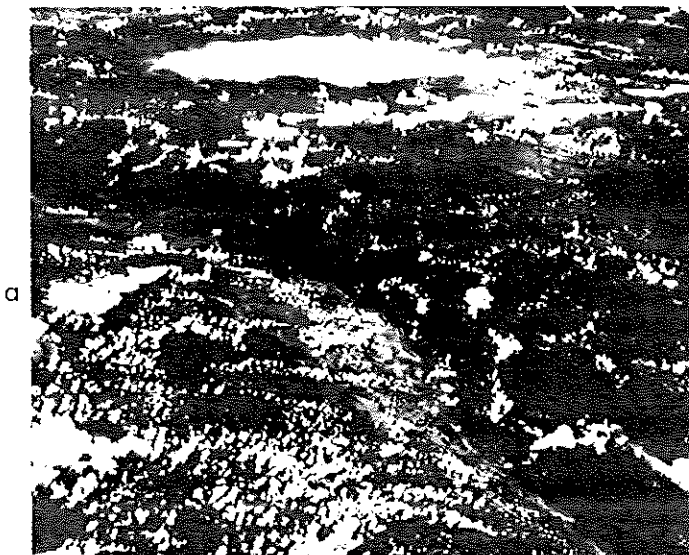


Figure 1a. Hexagonal "open" cells north of Cuba, photographed from Gemini 5 at 1827 GMT August 23, 1965.

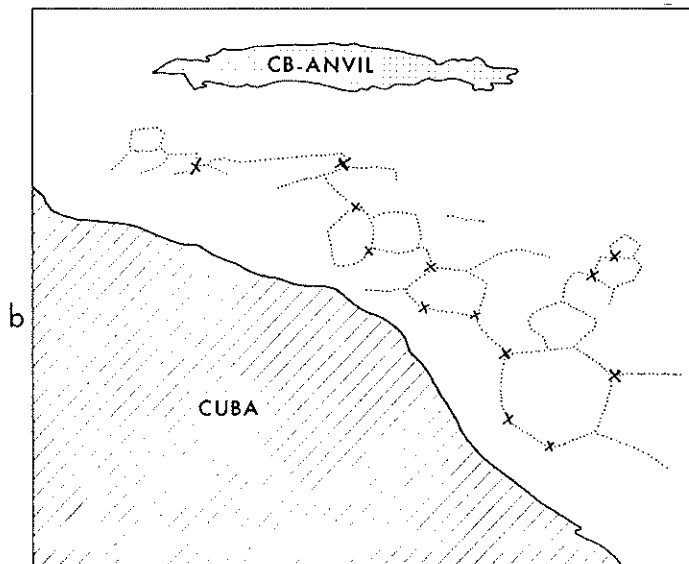


Figure 1b. Same-scale sketch of features on 1a. indicating cells and enhanced convection at cell corners (X).

Figure 1c. Theoretical distribution of vertical velocity in a Bénard cell from Pellew and Southwell [20]. Values of isopleths are w/w_o , where w_o = upward vertical motion at center.

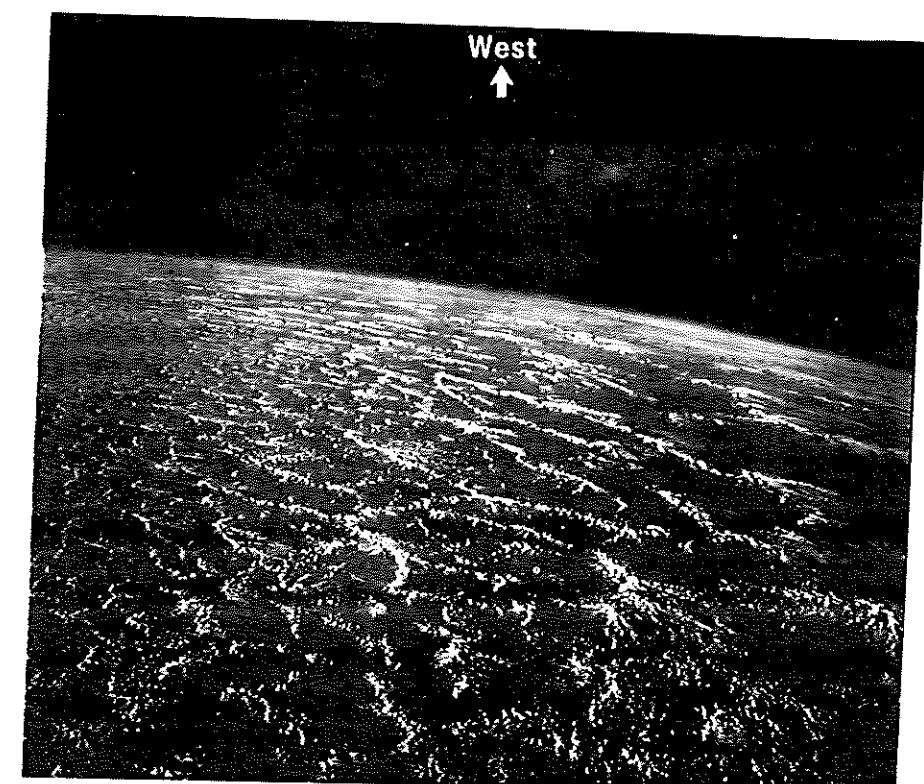
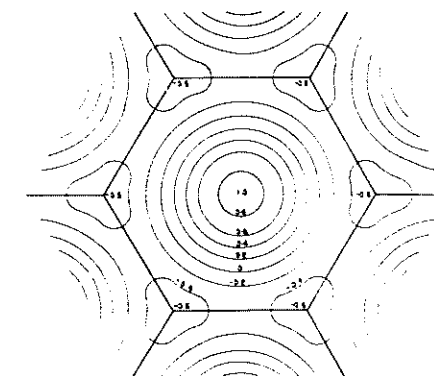


Figure 2. Irregular open cells photographed at approximately 20°N , 20°W from Gemini 6 at 1223 GMT on December 16, 1965.

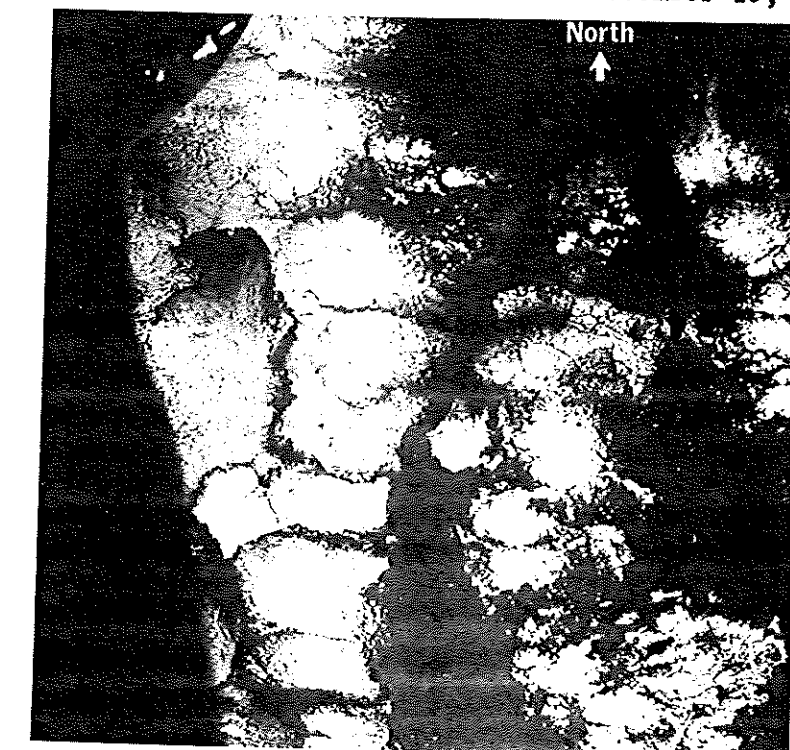


Figure 3. Closed cells southwest of the Canary Islands photographed from Gemini 6 at 1042 GMT on December 16, 1965.

An example of closed cells is shown in figure 3. These also are small, and the clear walls were so narrow they would have been unresolved by TIROS television pictures.

Picture Interpretation and Measurement

The problem of identifying closed cells on satellite television pictures is perhaps more difficult than identifying open cells because the cloudless cell walls are sometimes unresolved (see fig. 3). Low resolution could also obscure open cells (for example fig. 1), but there appears to be a scale-frequency characteristic that favors detection of open cells that may operate as follows.

A very frequent size range of cells is 20 to 100 km. The cellular nature of the mesoscale convection tends to produce narrow cell walls and a larger interior region. If the closed cells owe their characteristic appearance to descent in the cell walls and general ascent throughout the interior, the descent area could be very narrow, limited perhaps only by the turbulent mixing in stable air between adjacent cells, as illustrated in the sketch, figure 4.

By contrast, the open cells appear as rings of clouds which might be due to descent throughout the cell interior and ascent in the cell walls. The cloudy cell walls, being composed of many cumulus elements, have a width minimum that will be larger than the "descent-cell walls" because of the characteristic size of convective clouds.

If this explanation is valid, it follows that some areas of strato-cumulus clouds which appear to be overcast on satellite pictures are actually unresolved closed cells. The closed cells that are resolved may therefore be those in a dissipating or transitional state where the cell walls are abnormally wide.

The attempt has been made to determine accurately the cell size in each pattern by estimating the diameters of a representative sample, usually about thirty individual cells. This was done by stepping off the cell diameter over two degrees of latitude of the superposed geographical grid. Although distances were estimated to the nearest nautical mile and later converted to the nearest kilometer, the measurements are not actually that accurate, for many cells are elongated and irregular so it was necessary to use an "average" diameter. Moreover some open cells are not completely bounded by cloud walls; but if a corner suggested a dissipating wall, the invisible side was extrapolated to close off the cell.

The closed cells present a different measurement problem. Due to the uncertainty of cell wall location, distances were measured between the adjacent centers of the bright interior region. If every cell interior were identified, the center-to-center distance would be an accurate measure of the cell diameter. Were these cells in the dissipating stage so that some cell centers had vanished, however, the measured distance might span two cells, thereby biasing the measurements.

Satellite Pictures and Associated Data

Figures 5 through 26 are TIROS pictures of cells and their associated data. They are arranged to present like cases consecutively, not in chronological order.

These cases are a representative sample, but by no means exhaust the available cases for study. Patterns of convective groups in various stages of open cell organization appear in every outbreak of cold air over warm ocean, and the subtropical anticyclones generate both types in their subsiding regions. Closed cells also form in cold air as it moves equatorward and approaches equilibrium with the underlying surface.

The upper air soundings in this section reveal a range of conditions from strong subsidence inversions to deep moist layers. Both open and closed cells of oceanic anticyclones are associated with subsidence inversions, but open cells in cold air have been observed without any appreciable stability in the low troposphere. Figures 6b, 8b, and 12b (Lerwick) are examples of the latter.

The suggestion is developed in the next section that mesoscale cells depend, in part, upon the cumulus-scale turbulent mixing, and it is plausible that the mesoscale cells are confined to the convective layer beneath subsidence inversions. Where no inversion exists, cumulus development is frequently limited by entrainment and evaporation so it is also plausible that mesoscale convection is confined to the lower convective layer, even if no inversion exists. The open cells of figures 5, 7, and 11 are believed to be so confined.

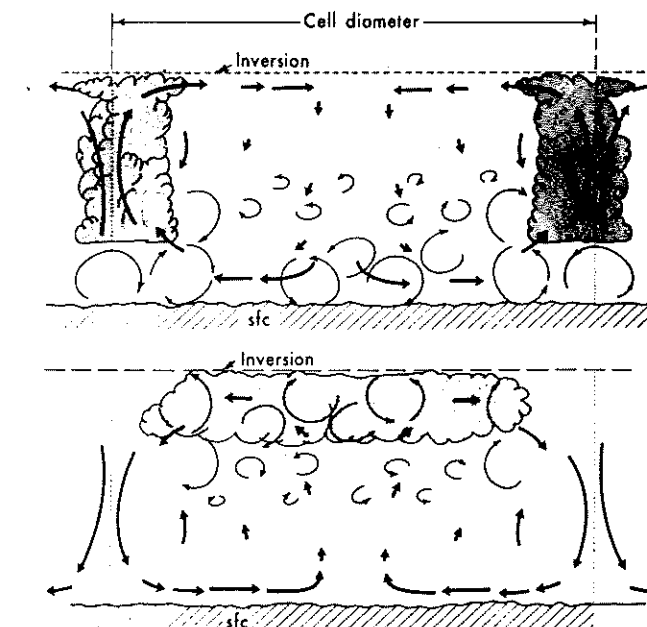


Figure 4. Cross section of open and closed cells. Mesoscale cellular circulation in heavy arrows, turbulent motion in light arrows. Large diameter eddies-strong mixing, small eddies-weak mixing.

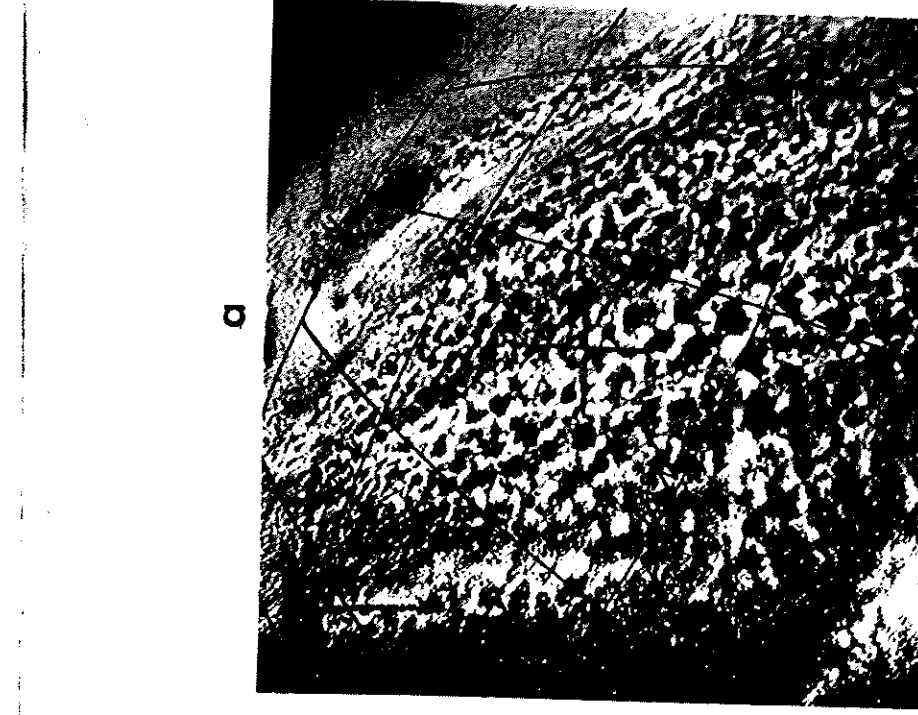
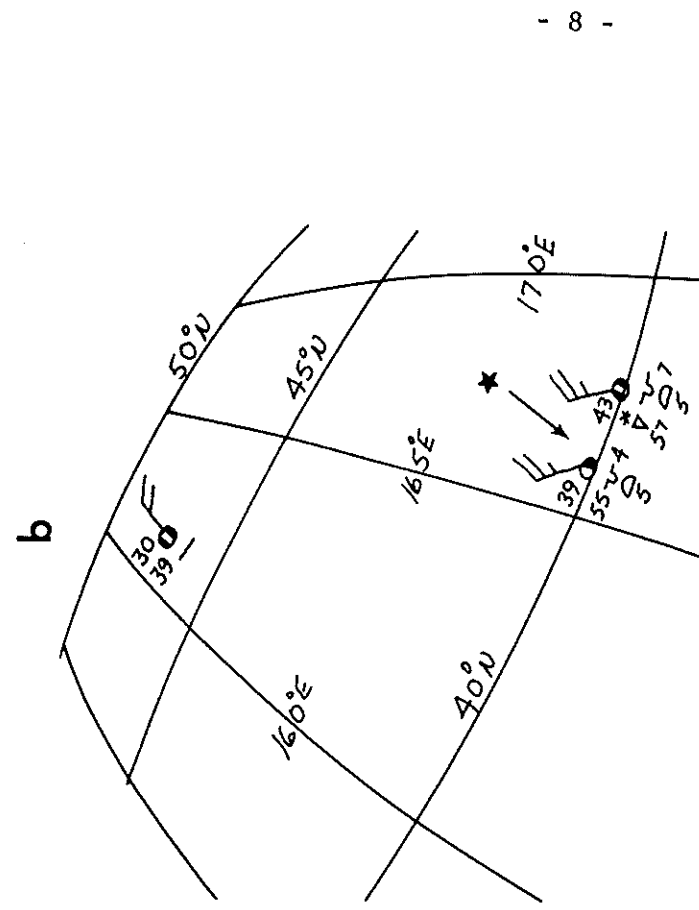
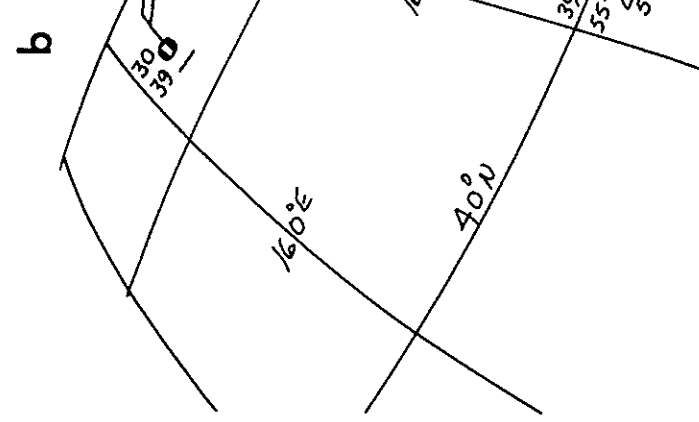


Figure 5a. Open cells in stratocumulus and swelling cumuli. Cell diameters range from 18 km. to 58 km., median size 35 km.

a

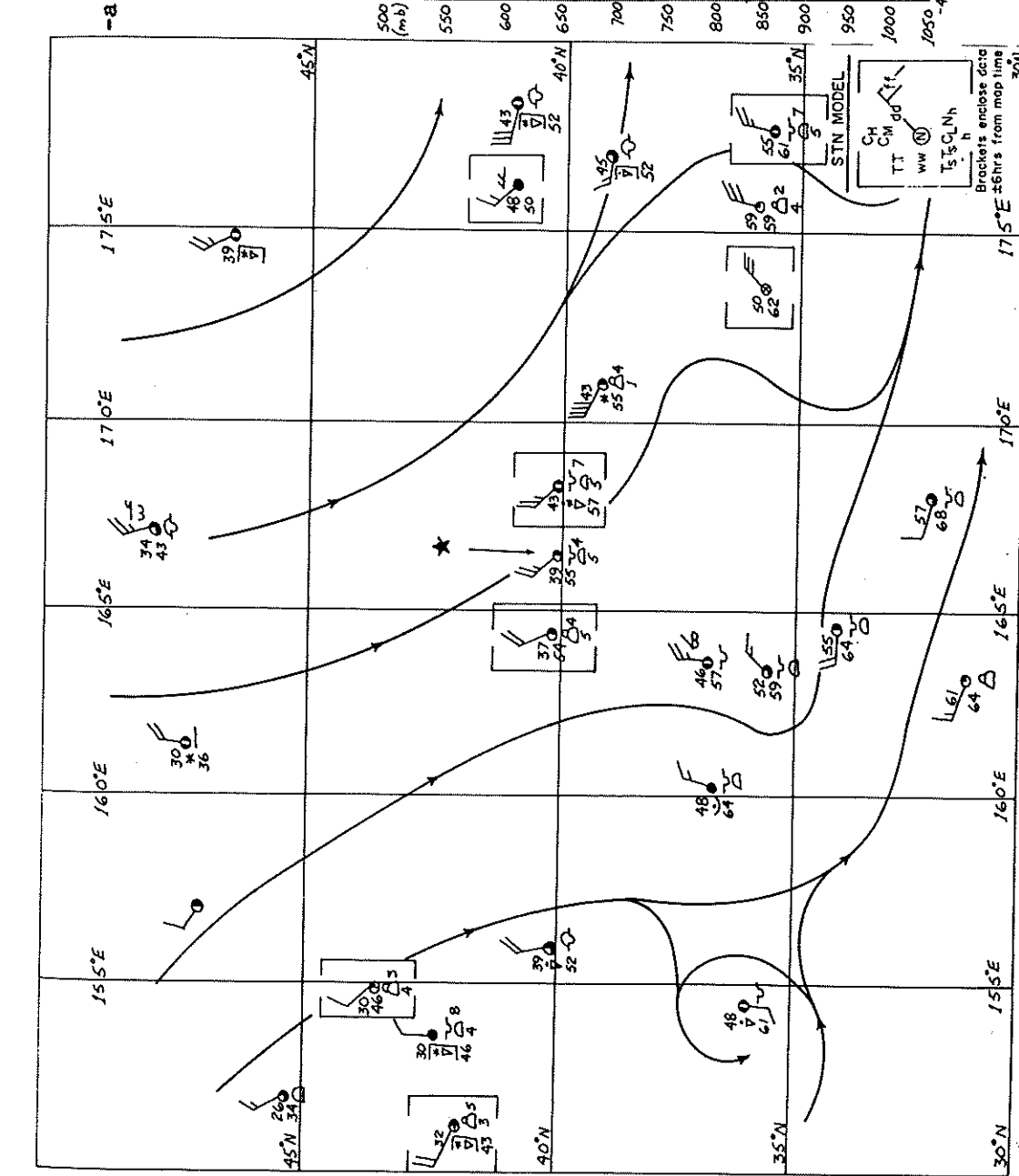


T-VII 3040/3040 0120GMT 11 JAN 64

Figure 5a. Open cells in stratocumulus and swelling cumuli. Cell diameters range from 18 km. to 58 km., median size 35 km.

Figure 5b. Same-scale grid with surface data (see fig. 6). Star indicates location of radiosonde.

- 8 -



- 9 -

Figure 6a. Surface map with streamlines for 00 GMT January 11, 1964.

Figure 6b. Ship's radiosonde at star position (see fig. 5).

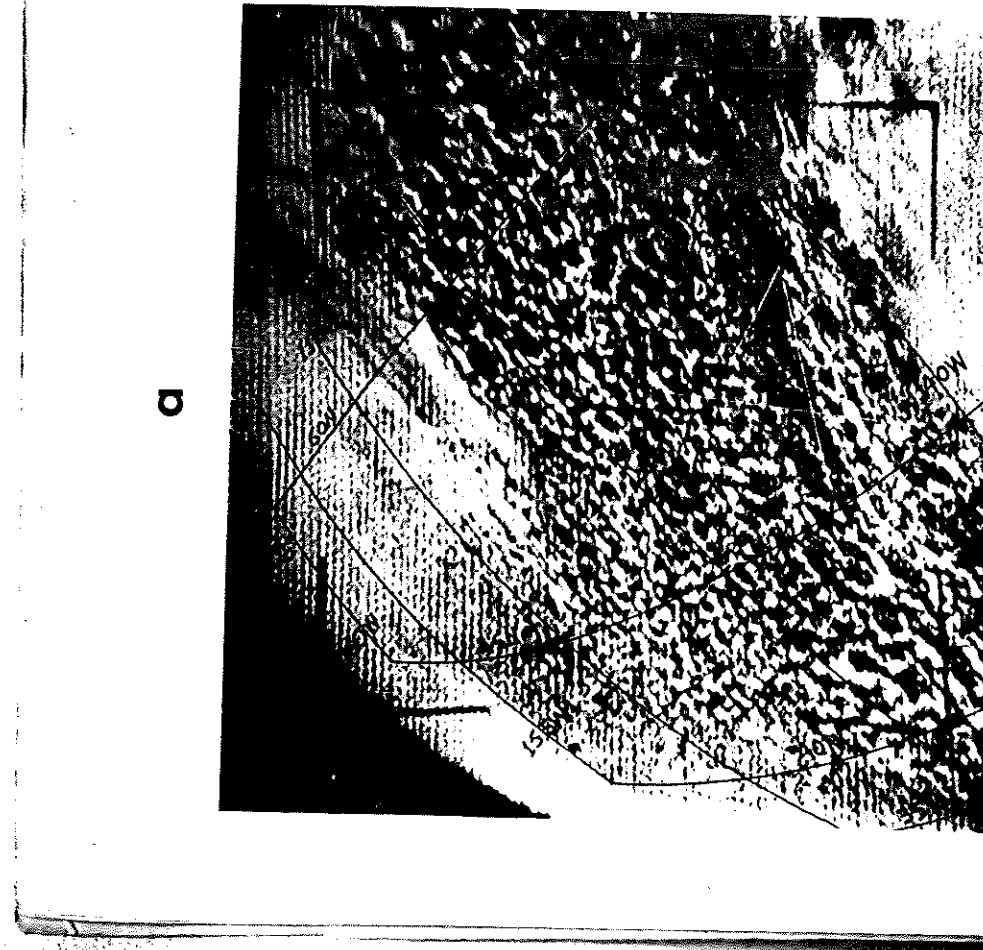
b

KFQJ 40.2°N 166.1°E

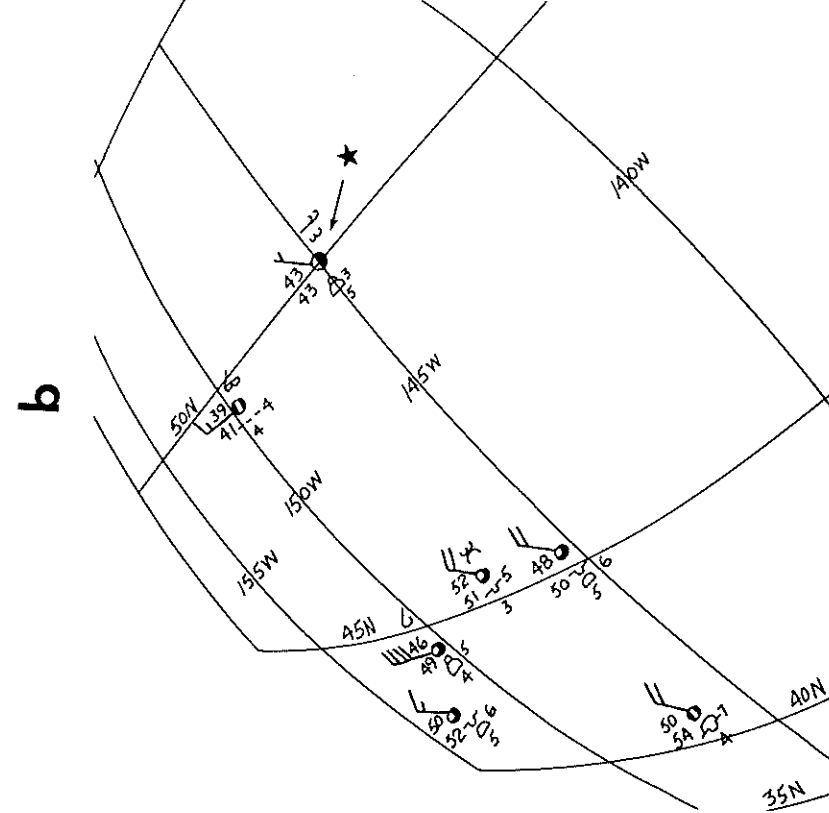
0000GMT 11 JAN 64

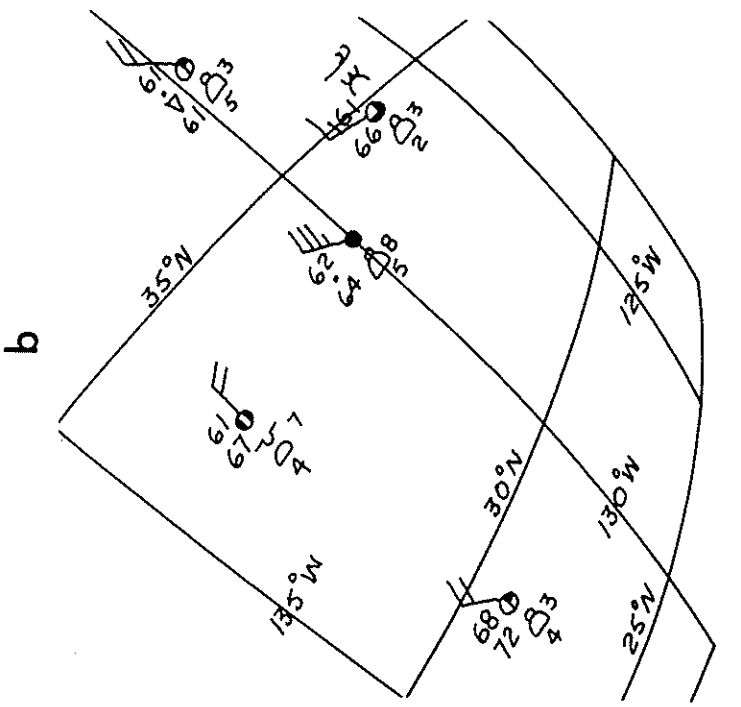
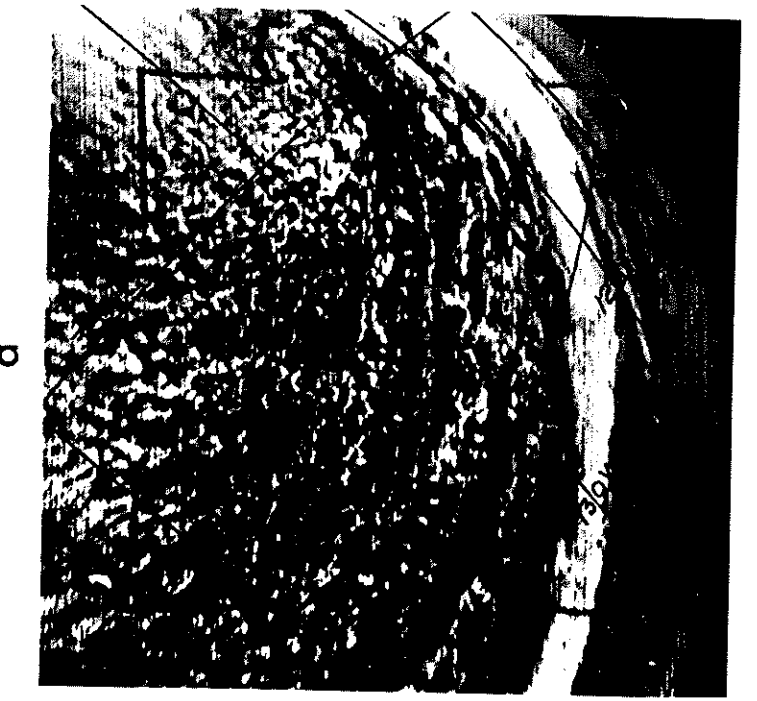
Brackets enclose data ± 6 hrs from map time

300



a



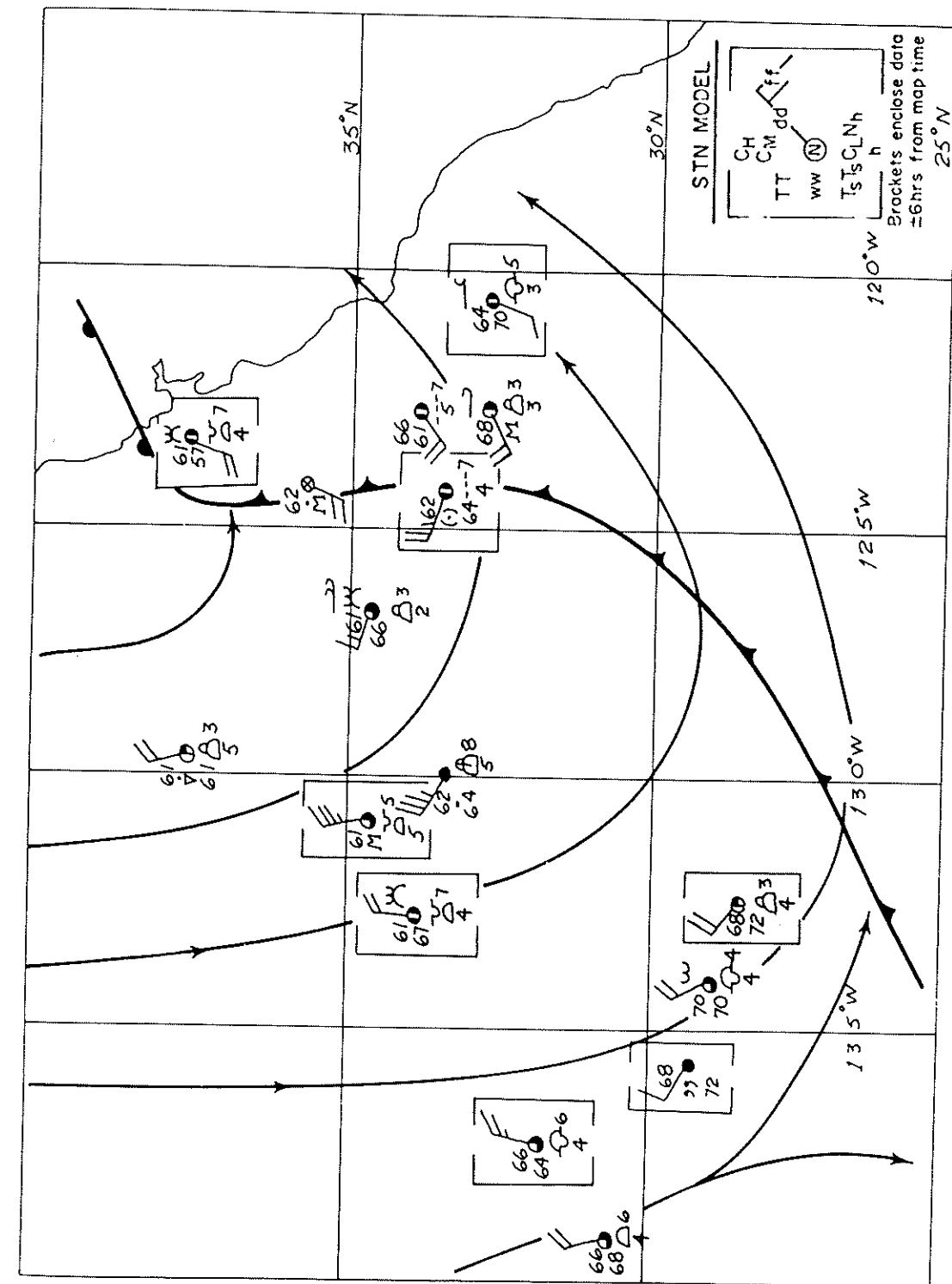


T-VII 2269/2268 2040GMT 19 NOV 63

Figure 9a. Open cells mostly in cumuli, behind an old cold front whose cloud band curves across bottom of picture (see fig. 10). Cell diameters ranged from 20 to 58 km. with median of 37 km.

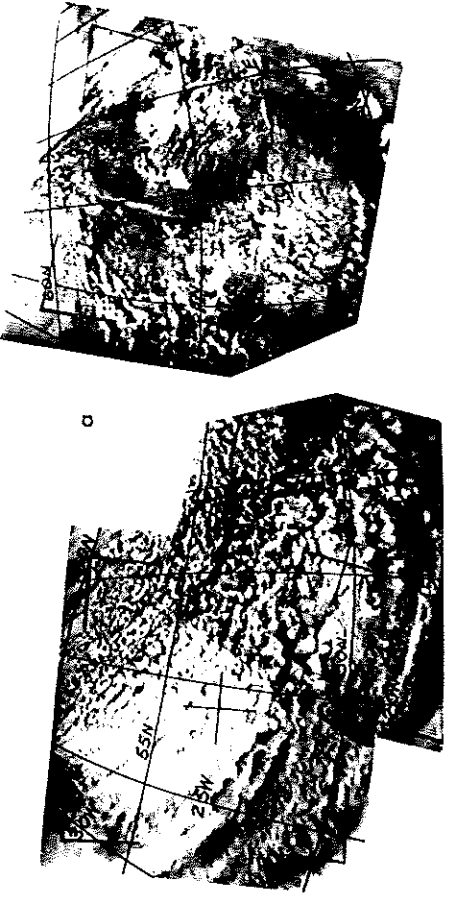
Figure 9b. Same-scale grid with surface data (see fig. 10).

- 12 -



- 13 -

Figure 10. Surface map with streamlines for 18 GMT November 19, 1963 (see fig. 9).



T-V 1277/1276 1310 GMT T-V 1276/1275 1130 GMT
16 SEPT 62

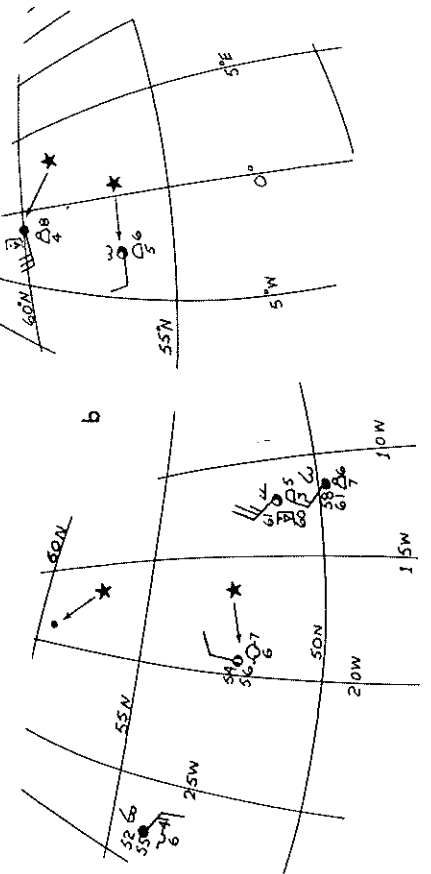


Figure 11a. Small open cells in cumuli along 59°N, 5° to 10°W from T-V 1276/1275 estimated to be 20 to 25 km. diameter. Two Picture mosaic from T-V 1277/1276 show open cells near 57°N., 20°W ranging from 35 to 55 km. with median diameter 42 km. (see fig. 12).

Figure 11b. Same-scale grids showing surface data and starred location of radiosondes.

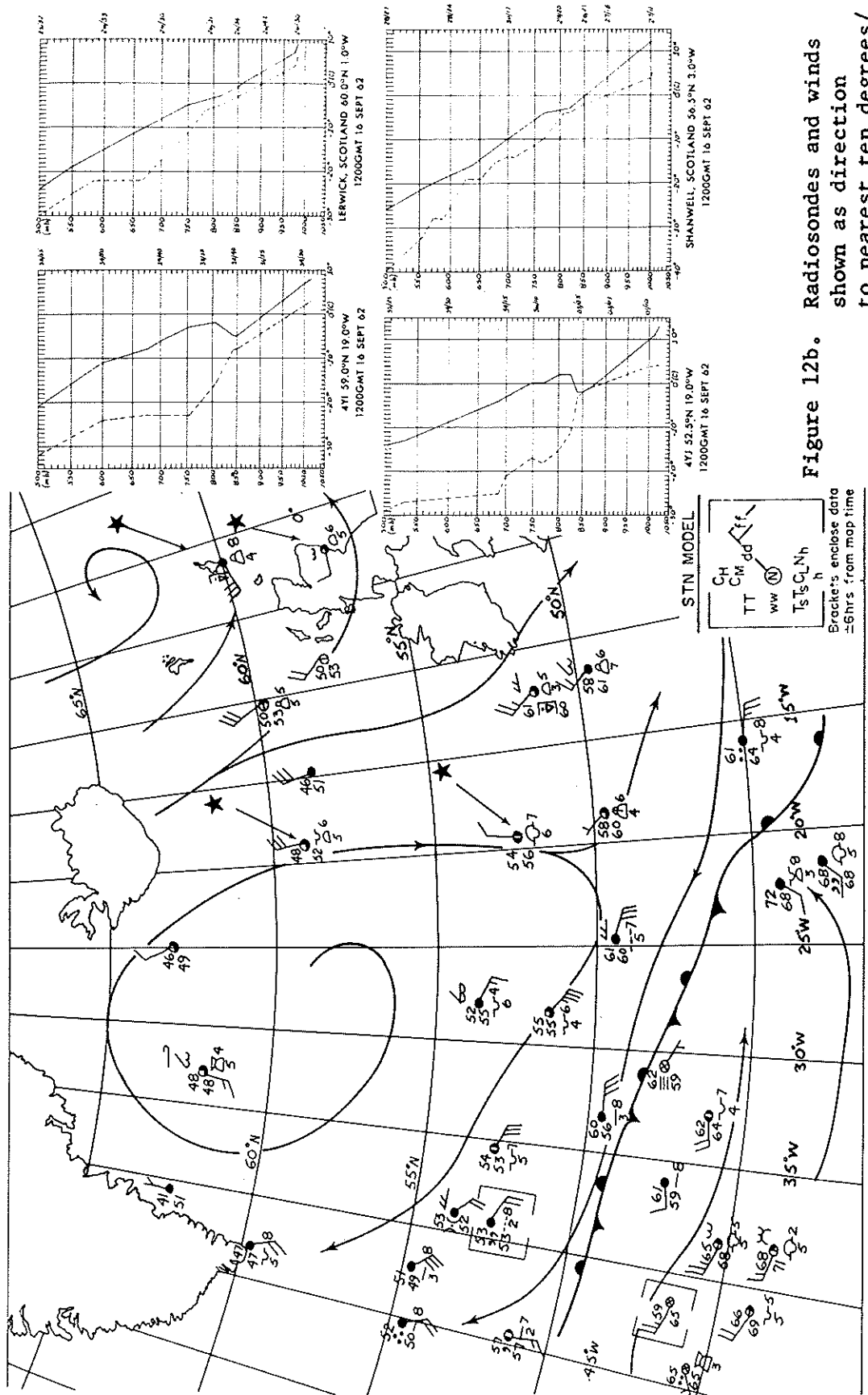


Figure 12a. Surface map and streamlines for 12 GMT September 16, 1962. Stars show location of radiosondes (see fig. 11).

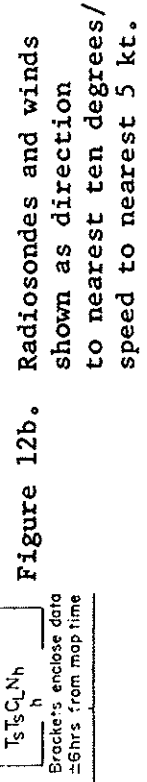


Figure 12b. Radiosondes and winds shown as direction to nearest ten degrees / speed to nearest 5 kt.

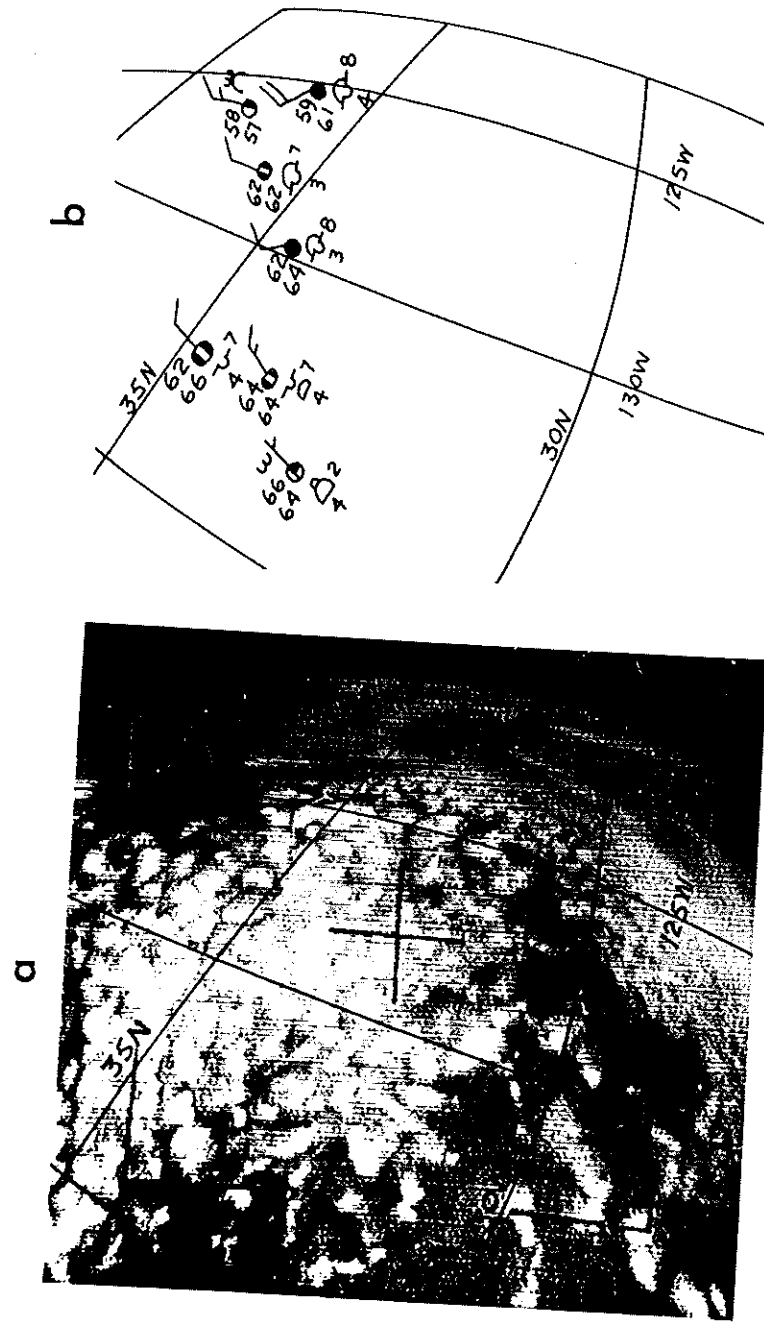


Figure 13a. Closed cells in stratus and stratocumulus (see fig. 14). Center-to-center distances range from 37 km. to 110 km. with median 72 km.

T-VI 4179D 2030GMT 1 JULY 63

Figure 13b. Same scale grid with surface data (see fig. 14).

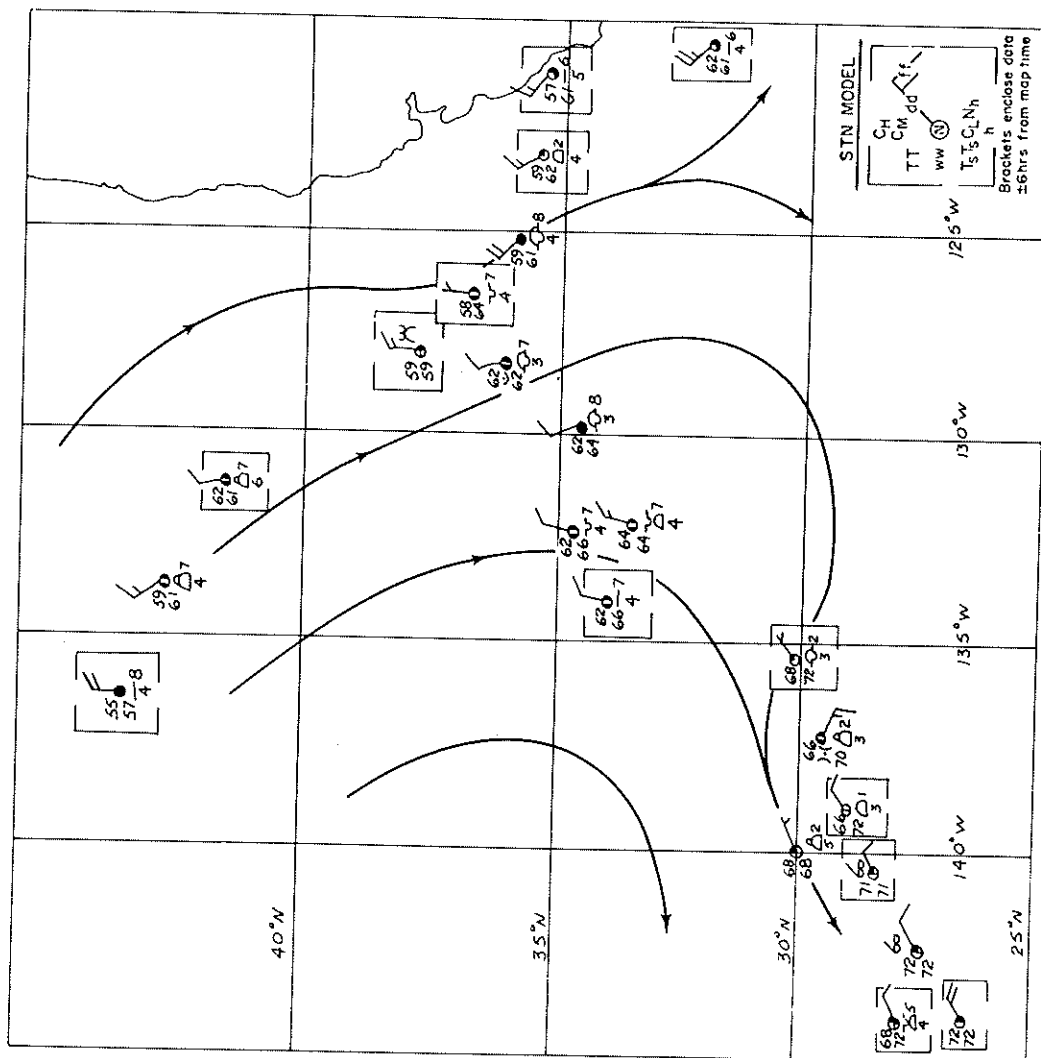
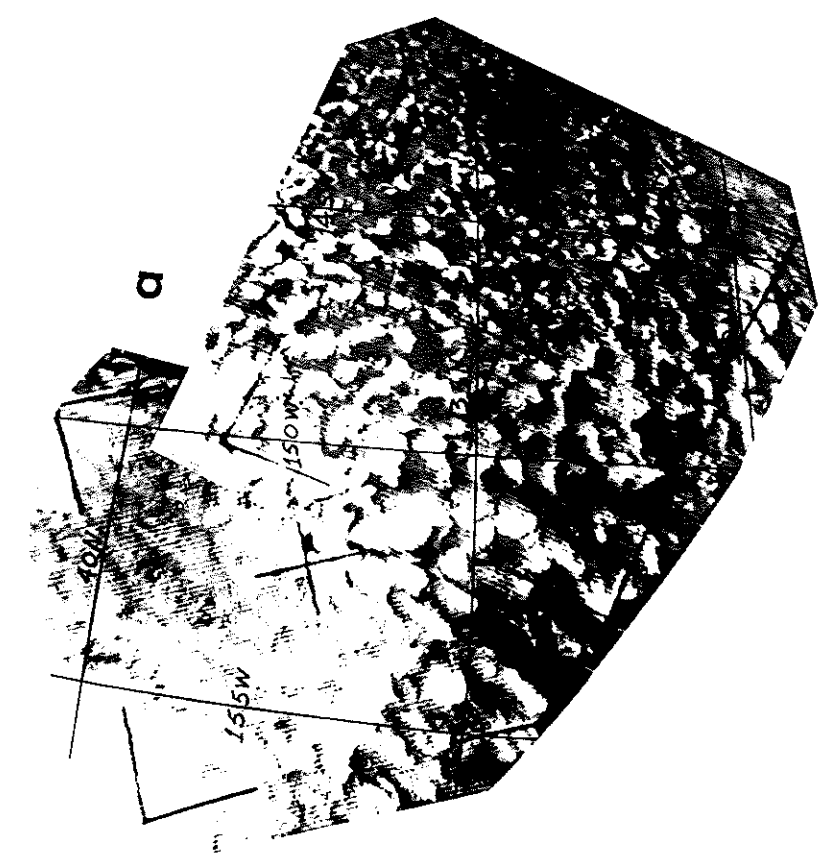
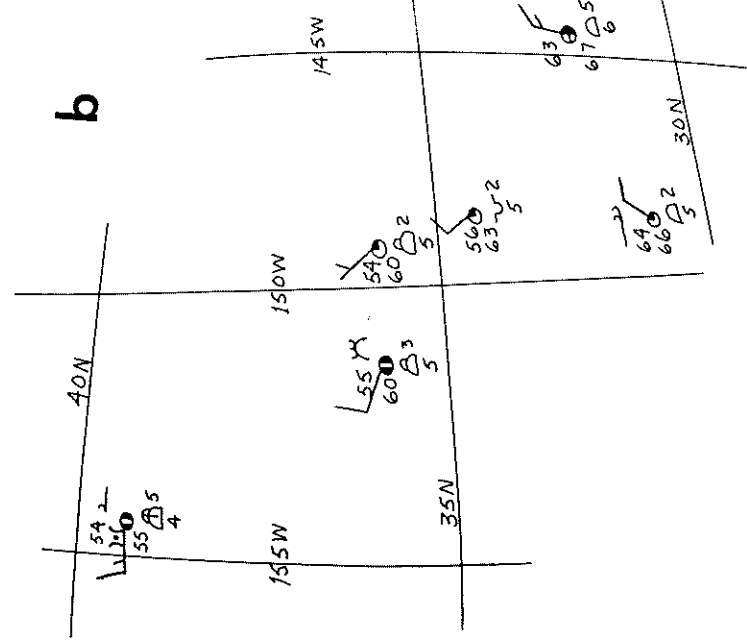


Figure 14. Surface map and streamlines for 18 GMT July 1, 1963 (see fig. 13).



b



T-IV 1004/997 2350GMT 18 APR 62

Figure 15a. Open cells in cumuli around 35°N, 145°W, ranging in size 41 km. to 113 km. with median diameter 70 km., and closed cells in cumuli centered around 37°N., 152°W; center-to-center distances 35 km. to 100 km. with median distance 63 km. (see fig. 16).
Figure 15b. Same-scale grid with surface data (see fig. 16).

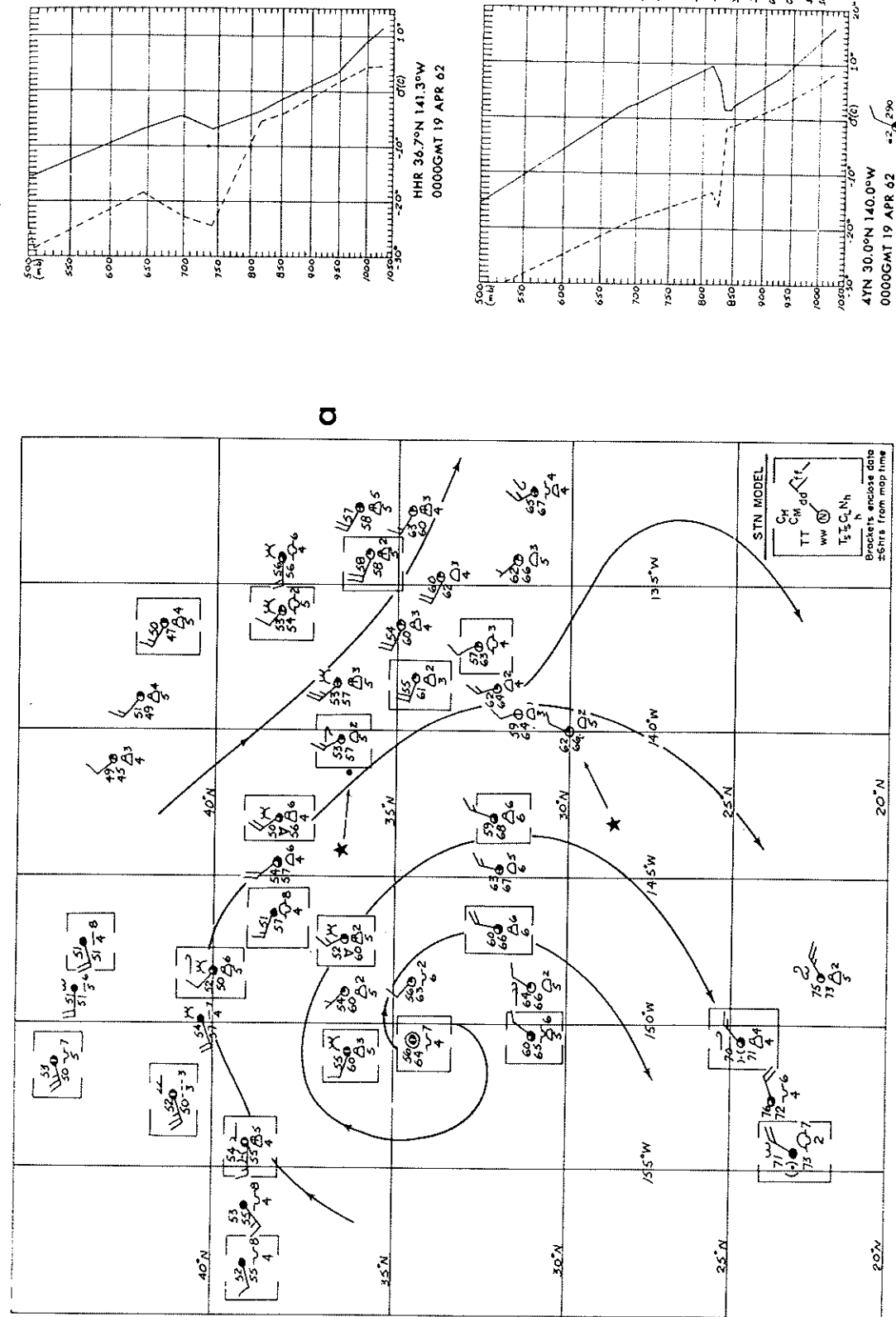
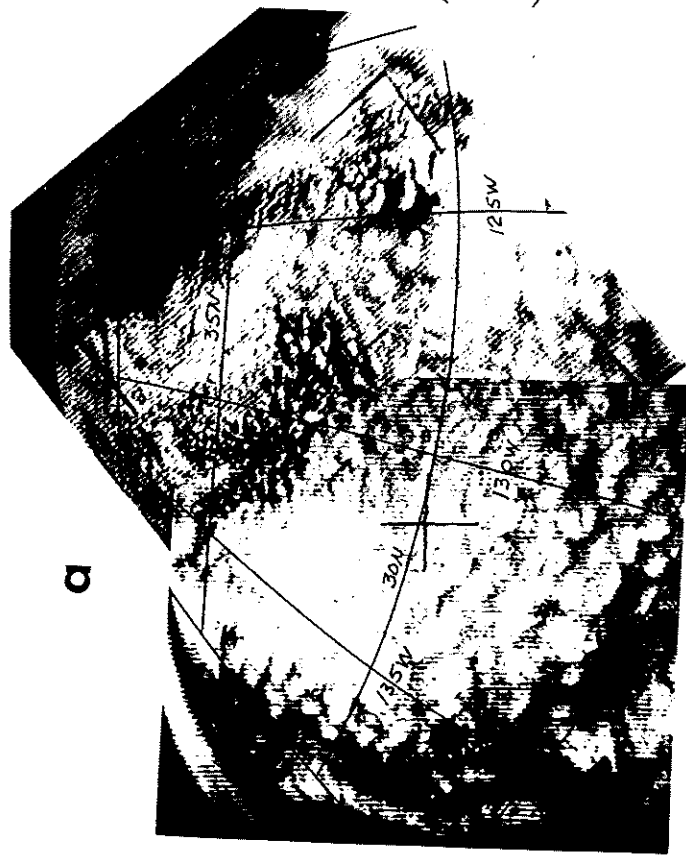


Figure 16a. Surface map and streamlines for 00 GMT April 19, 1962 and started location of radiosondes (see fig. 15).
Figure 16b. Two ship radiosondes taken immediately east of pictured area of figure 15.

b





a

b

T-IV 1685/1684 2120 GMT 5 JUNE 62

Figure 17a. Open cells centered around 35°N., 130°W. showed a size range 33 km. to 74 km., median diameter 43 km. Closed cells centered about 28°N., 133°W. had center-to-center distances 44 km. to 124 km., with median distance 82 km.

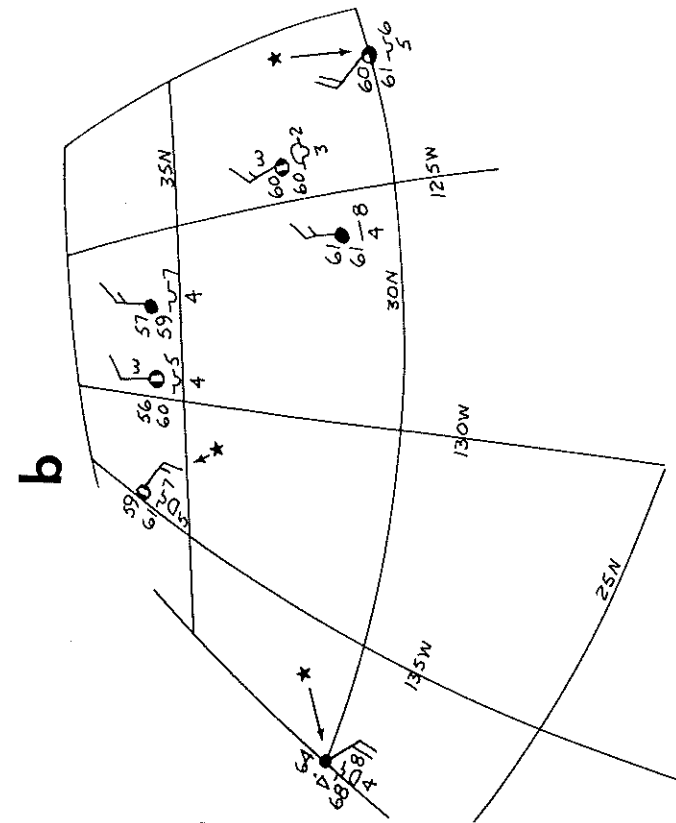
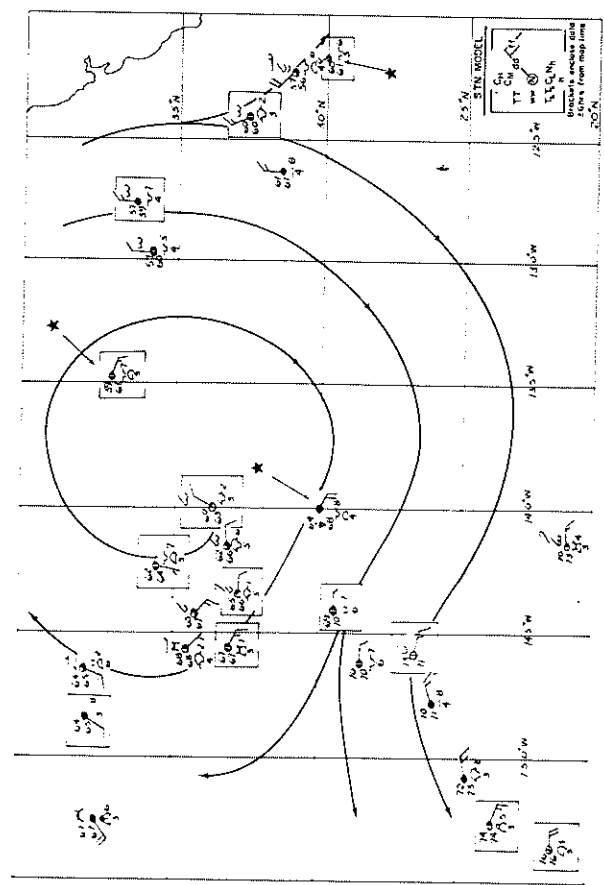
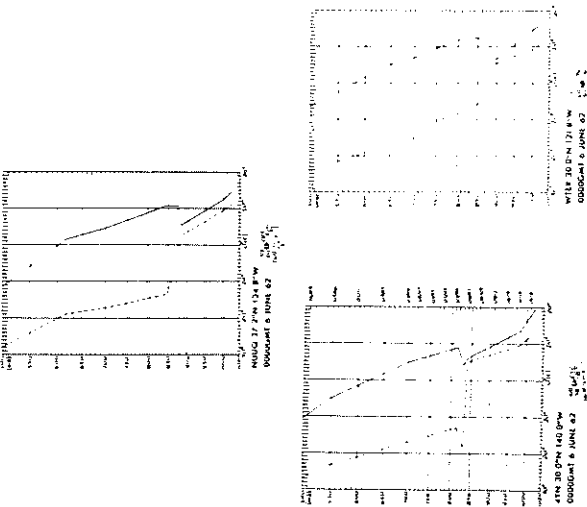


Figure 17b. Same-scale grid showing surface data and starred radiosonde locations (see fig. 18).



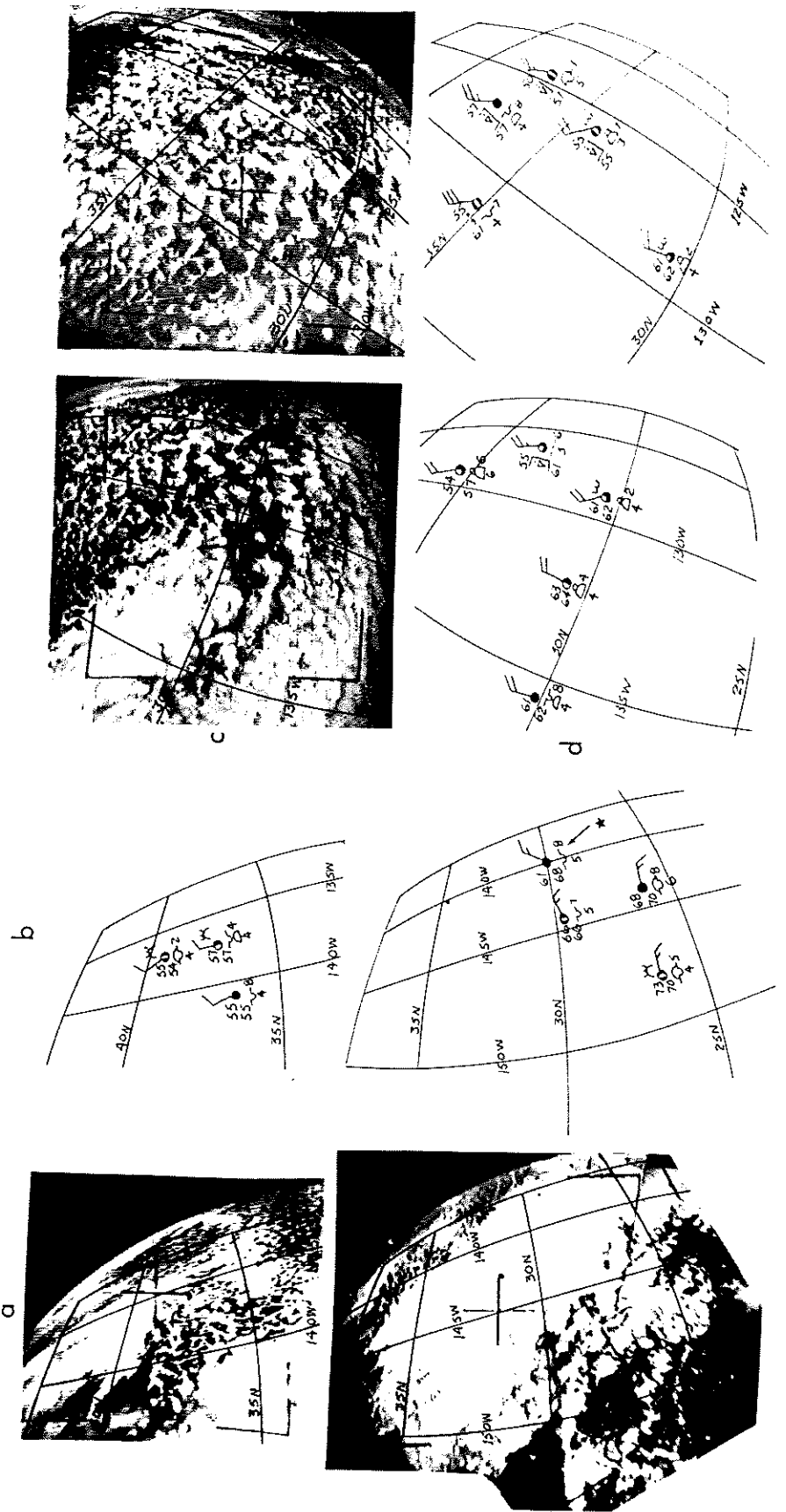
a



b

Figure 18a. Surface map and streamlines for 18 GMT June 5, 1962 and starred radiosonde locations.

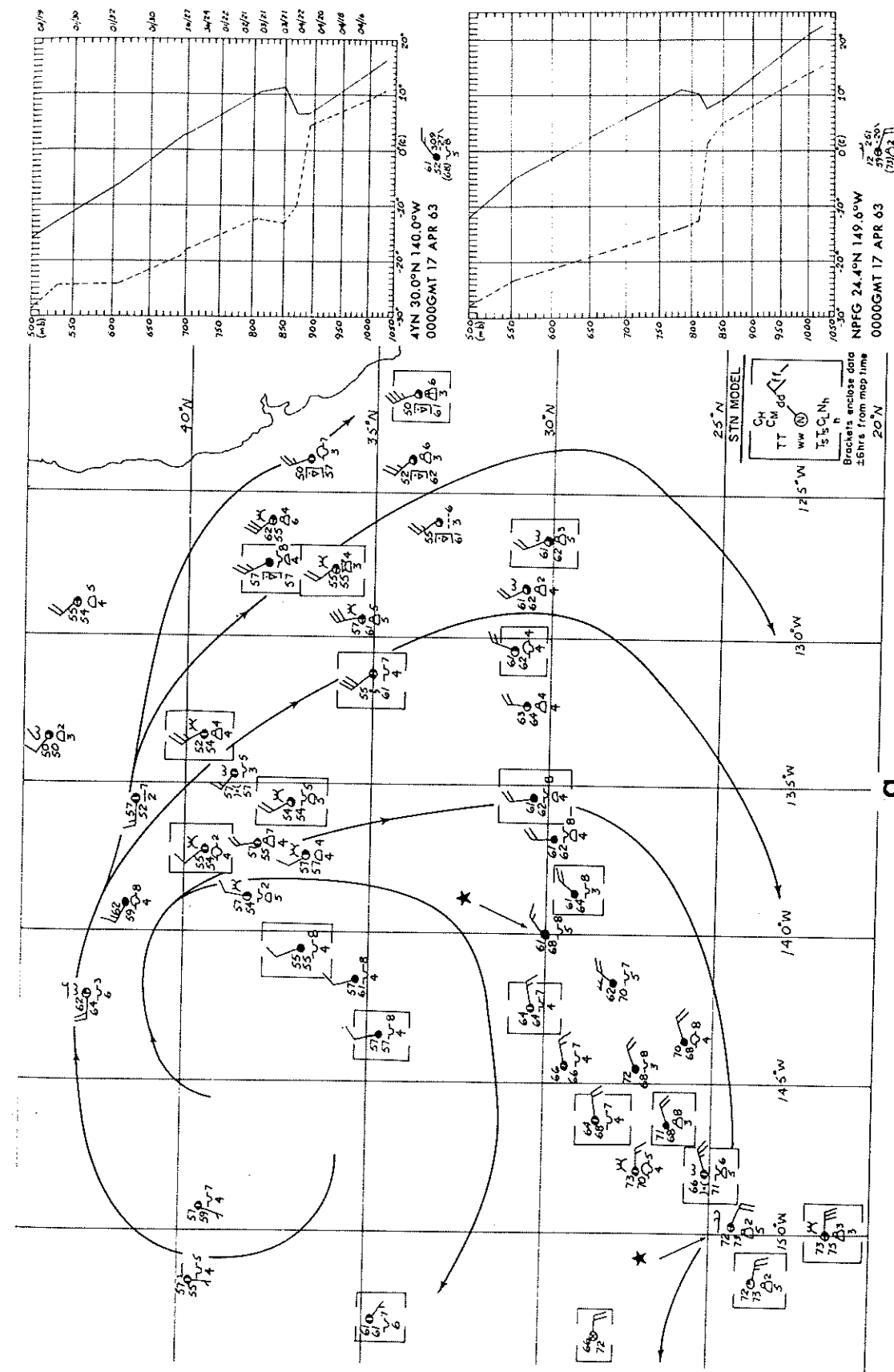
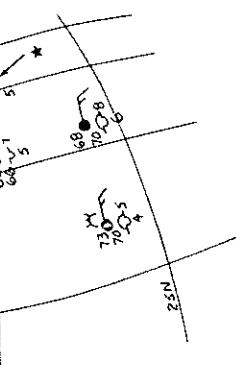
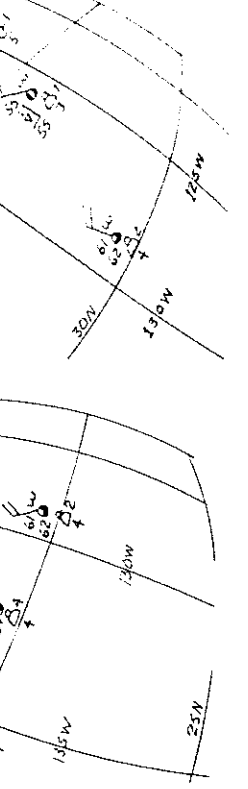
Figure 18b. Ship radiosondes and surface data. The easternmost sounding is in a broken area that shows a tendency for open cells but no size determination could be made (see fig. 17).



T-VI 4322/4321 2240GMT 16 APR 63

Figure 19c. Open cells in cumuli and closed cells in stratocumulus. Open cells 28°N. to 38°N., 125°W. range from 32 km. to 110 km., median diameter 56 km. Closed cells measured on left picture were included in sample measured for 19a.

Figure 19d. Same-scale grids with surface data (see fig. 20).



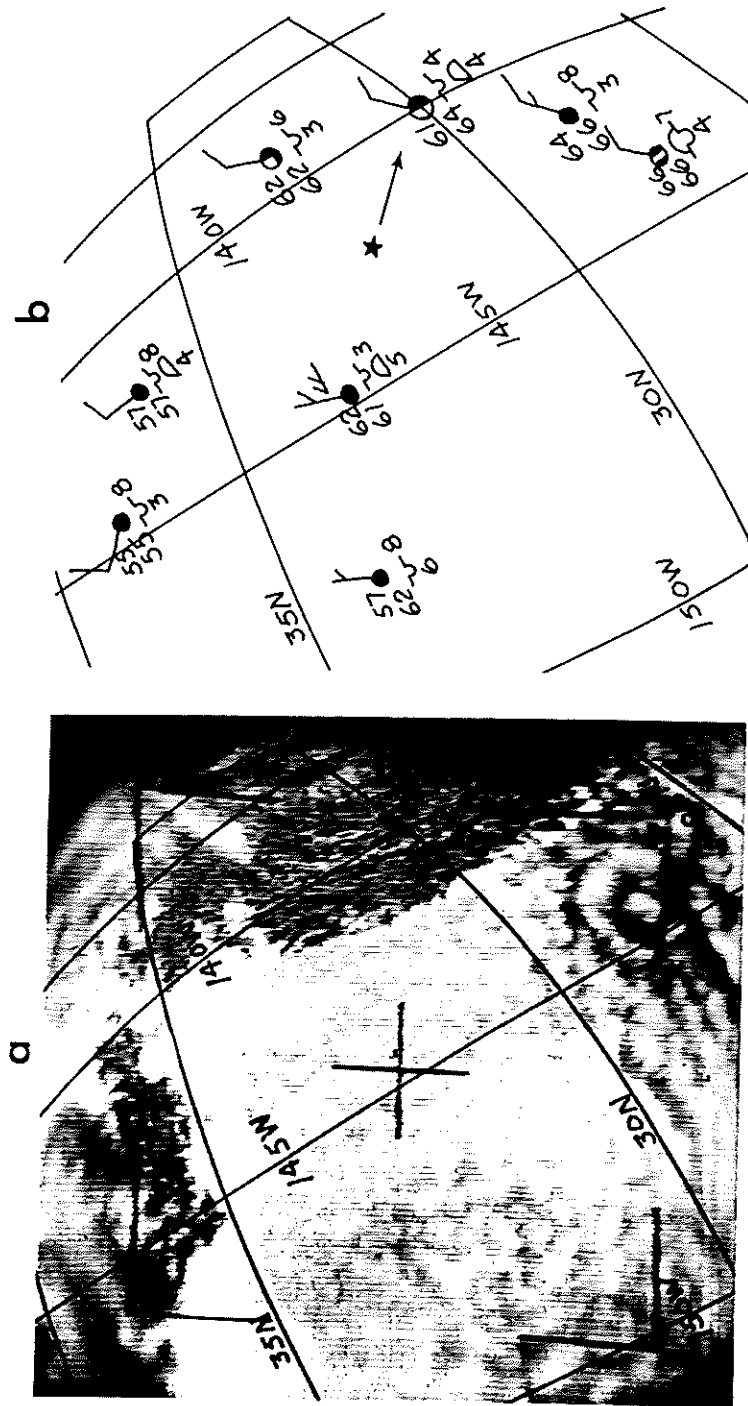


Figure 21a. Open cells centered around 30°N , 140°W . in cumuli estimated to be of uniform size about 37 km. diameter. Closed cells in stratocumulus range in center-to-center distances 32 km. to 70 km., with median distance 45 km.

Figure 21b. Same-scale grid showing surface data and starred radiosonde location (see Fig. 22). Figures 19 and 20 show the condition approximately one day earlier.

T-VI 3086/3085 2040GMT 17 APR 63

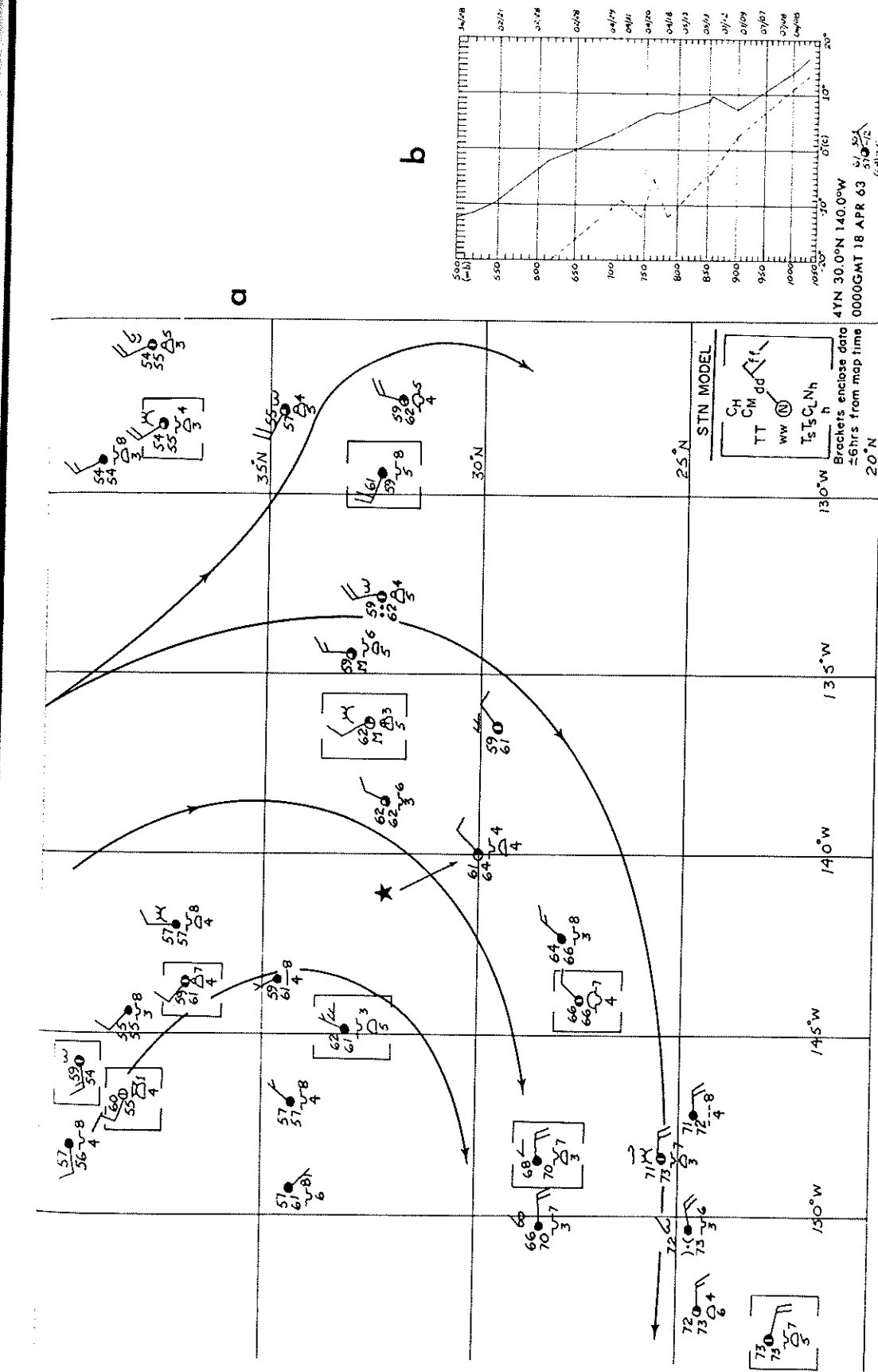
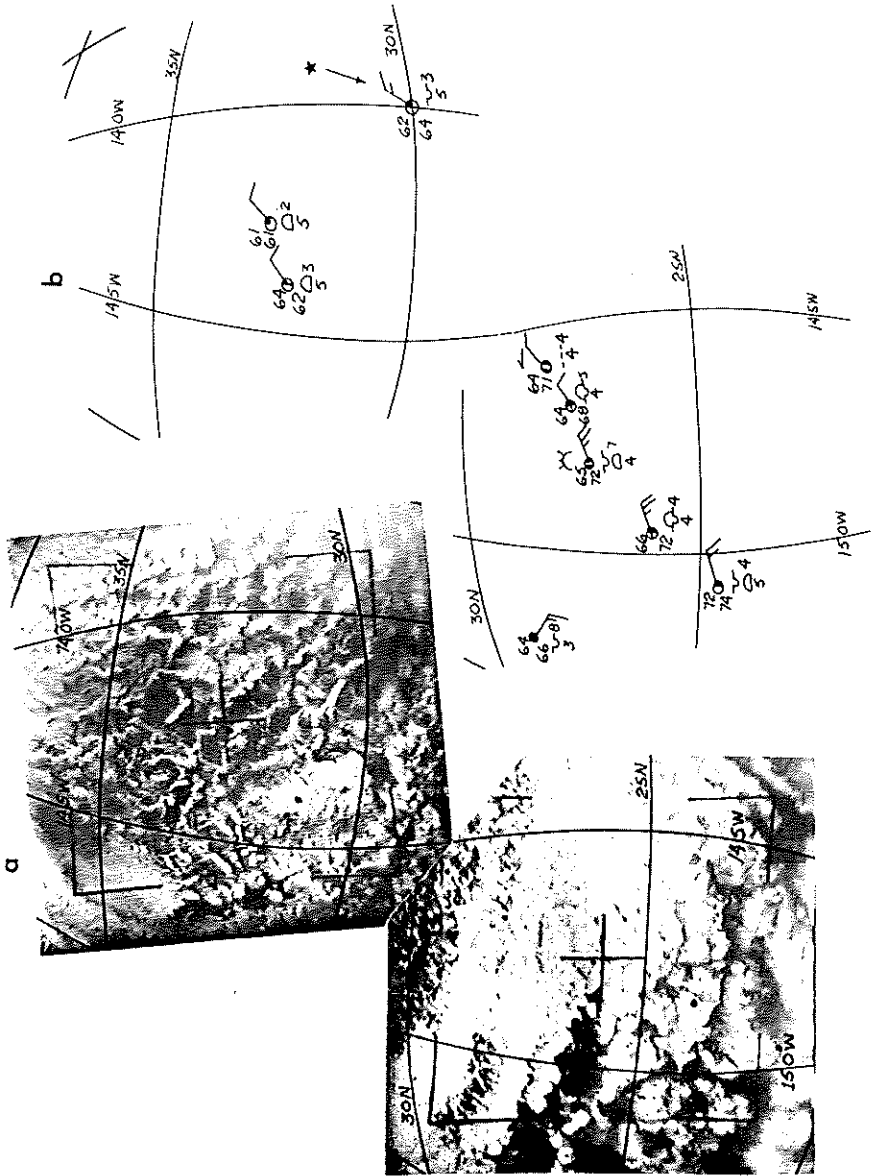


Figure 22a. Surface map and streamlines for 18 GMT April 17, 1963 (see Fig. 21) and location of radiosonde.

Figure 22b. Radiosonde and wind observation. Direction to nearest 10 degrees/speed to nearest knot.
Radiosonde.



T-VI 3202/3200 1750GMT 25 APR 63

Figure 23a. Open cells centered around 32°N , 143°W . Figure 23b. Same-scale grid showing surface in cumuli have size range 46 km. to 98 km. with median diameter 72 km. Closed cells near 25°N , 145°W . in stratocumulus have 27 km. to 58 km., range with median center-to-center distance of 48 km.

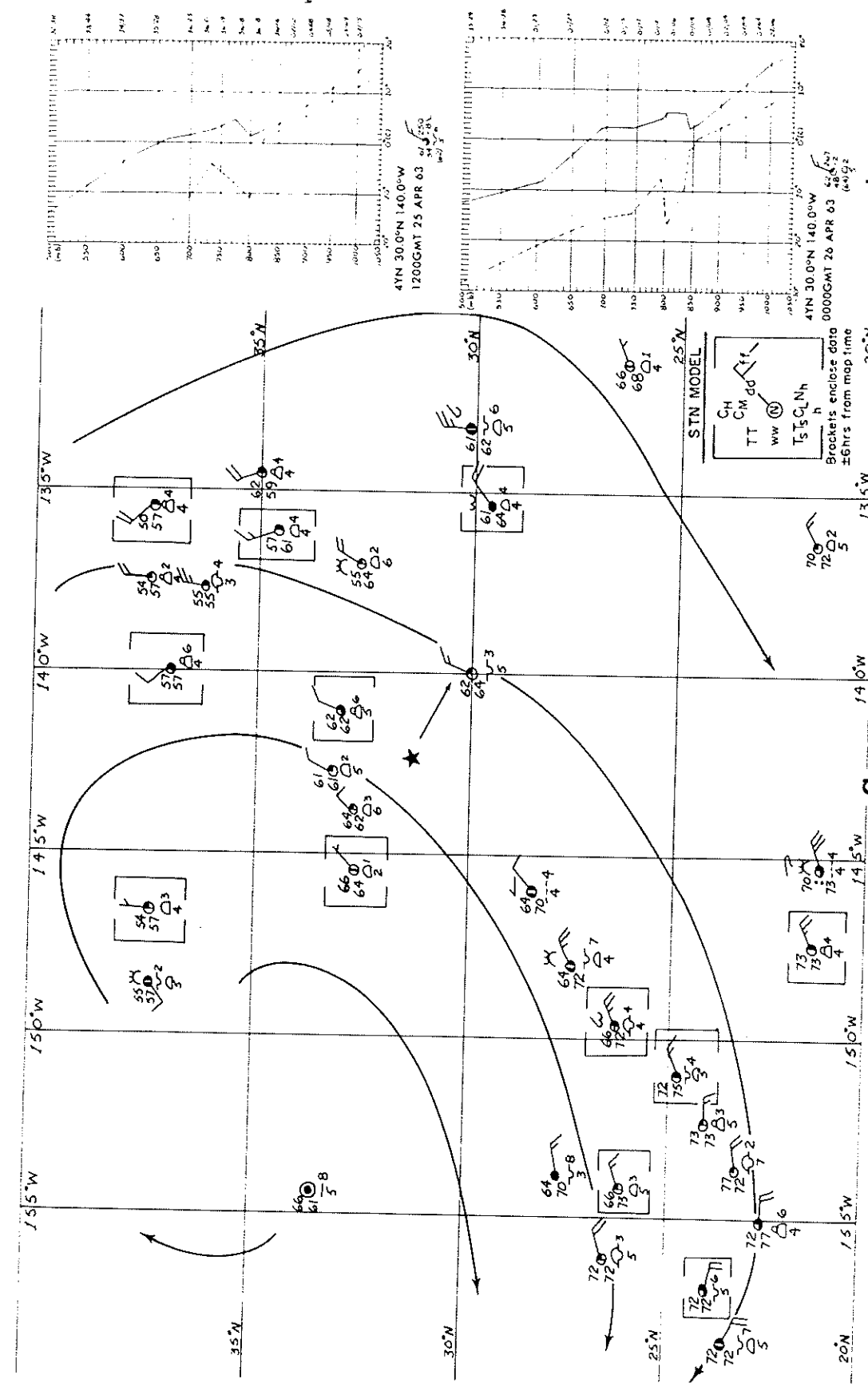


Figure 24a. Surface map and streamlines for 18 GMT April 25, 1963 and starred location of radiosonde. Figure 24b. Radiosonde and wind observation about 6 hours before and after picture, figure 23.

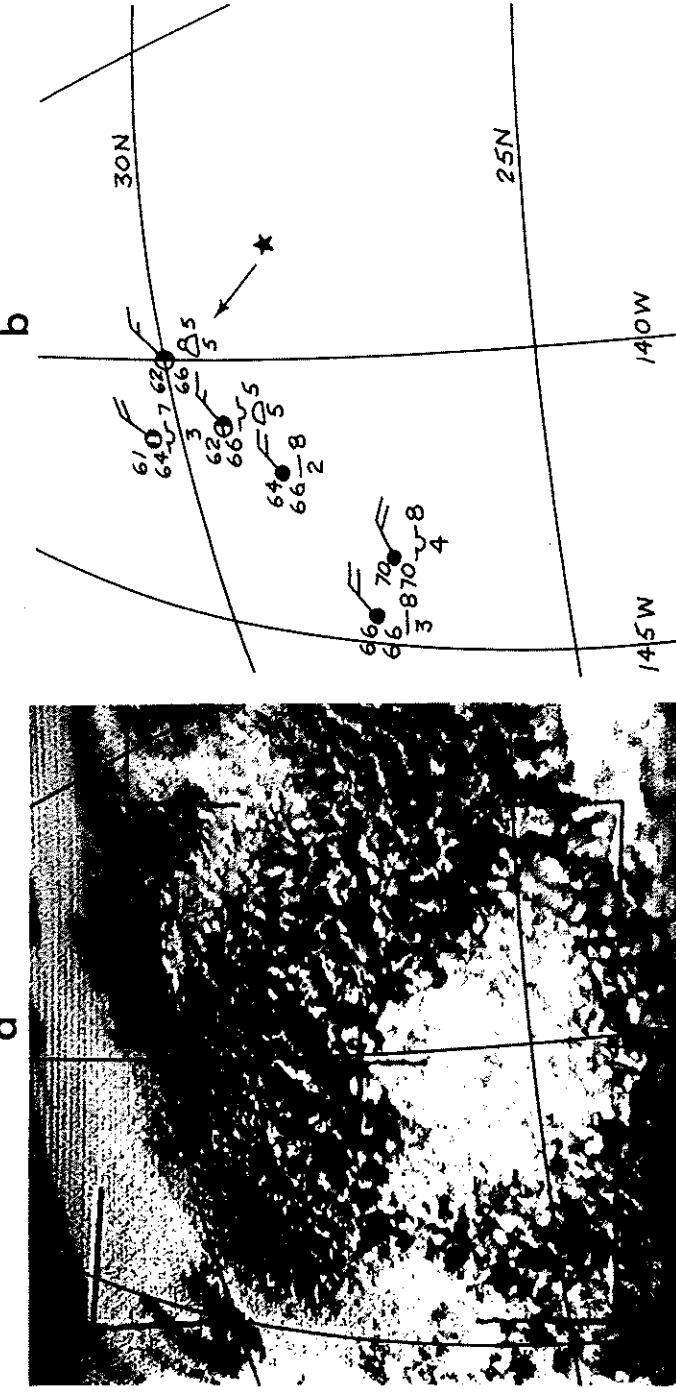


Figure 25a. Open cells in cumuli between 25°N. and 30°N. range in size from 20 km. to 74 km. with median of 37 km. The patch centered on 25°N., 140°W. appear to be a mixture of closed cells and thick-walled open cells (perhaps in transition) therefore no sizes measured. The cloud band across the top (background) is entirely ahead of the front (see fig. 26).

T-VIII 2080/2078 1800GMT 12 MAY 64

Figure 25b. Same-scale grid showing surface data and starred radiosonde location (see fig. 26).

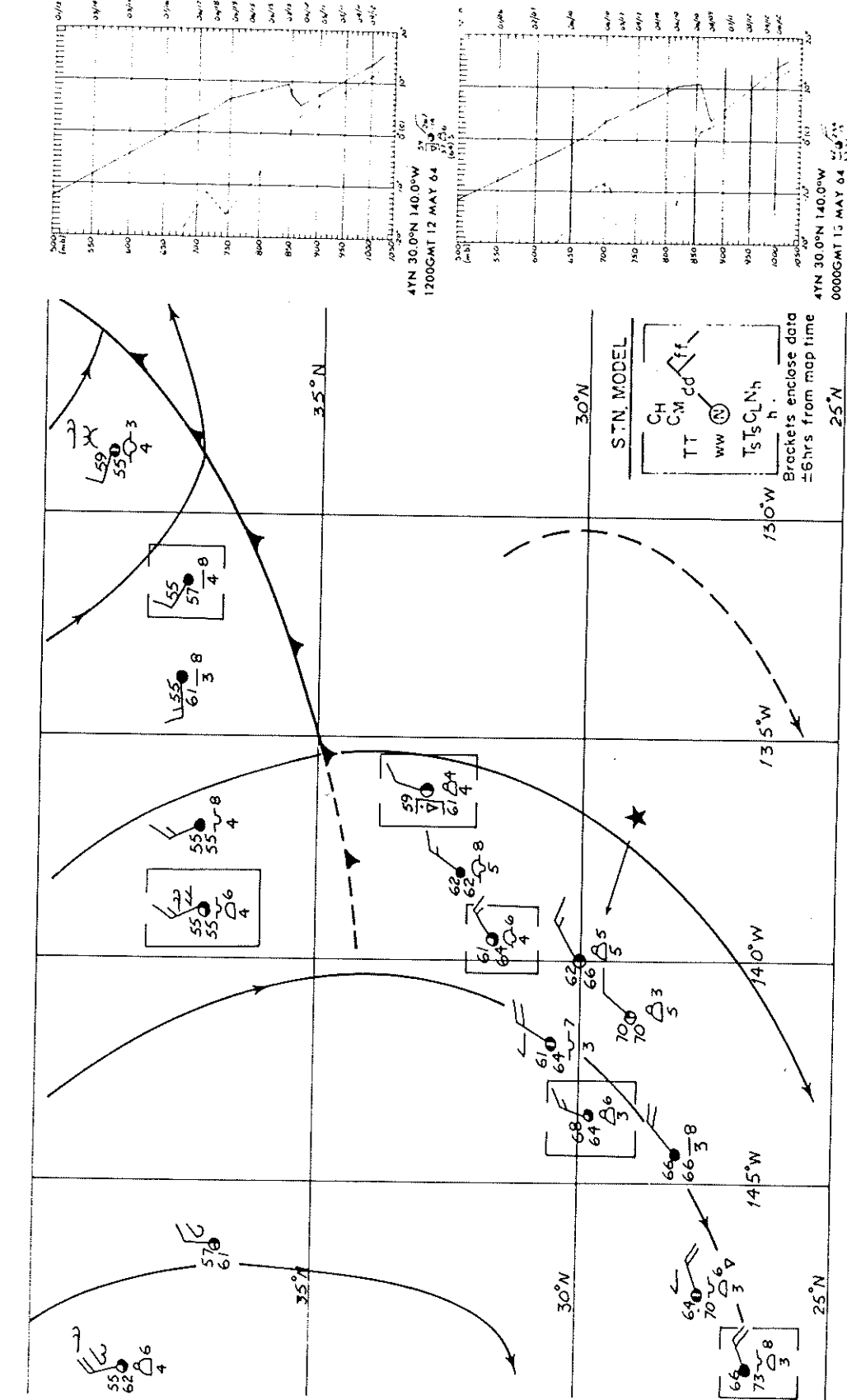


Figure 26a. Surface map and streamlines for 18 GMT May 12, 1964 and radiosonde location (see fig. 25). Figure 26b. Radiosondes and winds 6 hours before and after picture, figure 25. Winds direction to nearest 10 degrees/speed to nearest knot.

b

a

III. A HYPOTHESIS AND ITS THEORETICAL AND EXPERIMENTAL BACKGROUND

The fundamental phenomenon under consideration is the Bénard Cell and the many variations of convective patterns studied subsequent to Bénard's original work. The hypothesis presented here contends that the mesoscale patterns of clouds illustrated in Section II are the result of analogous cellular convection in the atmosphere.

Some striking differences are observed between atmospheric cells and laboratory-scale cells. It is hypothesized that these differences are the result of the differences known to exist between eddy turbulent processes in the atmosphere and their molecular counterparts in the laboratory. In addition to the contrasting magnitudes, the outstanding differences are (a) time and spatial variations of turbulent mixing and (b) its anisotropic nature compared to the small-scale molecular isotropy.

In the following paragraphs experimental and theoretical work is reviewed insofar as it is relevant to the empirical data concerning mesoscale cells. Reviews on the general subject of cellular convection have been written by Chandrasekhar [4] and Brunt [2], but in this section only those items are treated that, in the author's opinion, bear upon his hypothesis. The hypothesis is built on the less-than-solid foundations of incomplete data, physical intuition and analogy to results from the cited works. Almost no measurements of the necessary kind are available to test in the atmosphere the theories that are discussed in the cited literature, therefore none of the theory is discussed in any depth. The intent is merely to bring pertinent results to the reader's attention.

Direction of Circulation

Cells have been produced in the laboratory wherein the fluid descends in the (relatively) thin cell walls. Cells have also been produced where the walls are regions of ascent. Earlier writers considered the cell with descent in its center to have limited application to the atmosphere. They pointed to the cumulus cell as evidence: we don't observe doughnut-shaped cumuli! (Some middle cloud patterns were suggested as possible counterparts).

In contrast, the existence of both cell types is proposed here, and the central analogy upon which the author's hypothesis turns is the similarity between the laboratory and the atmospheric patterns. Figures 1, 2, and 3 are strong evidence that nature produces both types in the atmosphere.

No single factor has been shown to be the controlling influence of the direction of motion in laboratory cells--probably there is more than one such effect. Nakagawa and Frenzen [17] concede such a possibility. After describing the relation between direction and the choice of unstable boundary in a rotating fluid they concluded that if instability were induced "...in this ideal manner, the direction...would very probably either be completely arbitrary, or would be determined by some smaller effect such as the variation of viscosity with temperature."

A personal communication from Ruby Krishnamurti (U.C.L.A., Los Angeles) pointed out that the convective mode in the laboratory was also influenced by the time-change of temperature. The direction of circulation at proper Rayleigh Number could depend upon whether the mean temperature of the fluid was increasing or decreasing.

There is some evidence that both rotation and changing temperature are of secondary importance in the atmospheric case, if they apply at all:

- a. The influence of rotation on stability will be shown later to be negligible for layers only a few kilometers thick.
- b. Both open and closed cells exist where there is continued heating from the surface and the layer temperature is increasing.

Variation of viscosity as the largest influence on direction has great appeal in the case of mesoscale cells. This effect was suggested by Graham [9], explained intuitively by Stommel [27], demonstrated experimentally by Tippelskirch [29], and shown theoretically by Palm [18] and by Segel and Stuart [26]. Because this particular effect and its analogy with the atmosphere is central to the author's hypothesis, each of the works in the preceding sentence deserves discussion.

Graham [9], discussing his experimental work, showed that the fluid at cell center moved toward the boundary of highest viscosity once steady-state convection was attained. The viscosity of most liquids decreases with increasing temperature, whereas, gases exhibit the opposite response. Laboratory cells are always produced in fluid in which there is a temperature decrease with height. For that

reason, viscosity decreases with height when the working fluid is gas, and increases with height for most liquids. Accordingly, the circulation under proper conditions, is downward at cell center in gases and upward in most liquids.

Stommel [27] offers an intuitive explanation for this effect of viscosity, but it is not completely satisfying for reasons mentioned below in the description of the theoretical work. There is no apparent reason, however, why the effect could not be a contributing factor. He postulates that circulation direction will be favored which involves the smallest frictional loss. Implicit in his explanation is the assumption that the distribution of vertical motions is such that, due to decreasing area with decreasing radius, the radial speed along the lower boundary is greatest near the cell center and least near the walls. In a convecting gas (descent at the centers) the highest horizontal speeds involve the gas which has recently come from cooler portions of the cell and is therefore less viscous than the fluid which has moved farther along the hot boundary. Thus the highest speeds are associated with the lowest viscosity on the bottom boundary. Where liquid is involved (ascent in centers) the coolest fluid is near the walls where it has recently descended. This cooler, more viscous, liquid is associated with the lowest speeds, and as the radial inflow speed increases toward the center, the viscosity decreases. In both cases the circulation minimizes the viscous drag on the lower boundary.

An ingenious experiment by Tippelskirch [29] demonstrated the effect of this temperature-induced (vertical) variation of viscosity.

He produced Benard cells in molten sulfur. From its melting point near 110°C , up to 153°C , the response of viscosity to temperature is typical of liquids, that is, decreasing with higher temperatures. In the range of about 153° to nearly 200°C , however, the relationship reverses and the viscosity increases sharply with temperature. Benard cells with ascent at the cell center formed in the lower temperature range. Continued gradual heating carried the liquid into the higher temperature range, and the circulation reversed; descent then appeared at the cell center.

Palm [18], in a theoretical study of the tendency toward hexagonal cells, derived the result that the variation of viscosity with temperature could indeed produce the experimental results. Segel and Stuart [26] disputed some aspects of Palm's treatment, but they also concluded that the temperature-viscosity relationship could have the observed effect on circulation direction.

These results may not be precisely the workings of the effect suggested by Stommel. In both of these mathematical formulations, only the vertical gradient of temperature (and thus of viscosity) is explicitly modeled. It is not readily apparent that a horizontal gradient of temperature is involved, hence no horizontal change of viscosity along the lower boundary could influence the motion.

In any event there is convincing evidence that, under proper conditions, temperature-produced viscosity changes in laboratory cells can control the circulation direction. Preparatory to constructing the laboratory-atmosphere analogy, let us summarize the laboratory-theoretical results.

- a. Direction of circulation is initially away from the surface of greatest instability, but when steady-state convection has been achieved, this does not necessarily hold (Graham [9]).
- b. Direction of circulation, in steady state, may be determined by relative instability of the upper and lower boundary layers if significant rotation is present. If rotation is small, other factors may control direction (Nakagawa & Frenzen [17]).
- c. Direction of circulation, in steady state with no rotation, can be determined by the temperature-produced variation of viscosity in the vertical. Intuitive reasoning suggests that this might be due to circulation favoring minimum frictional losses (Palm [18], Segel & Stuart [26], Stommel [27]).

It is proposed here that the direction of circulation in mesoscale cells is determined by the vertical variation of eddy viscosity.

Further, it is contended that the open mesoscale cells are formed by descent at cell center (thus evaporating the clouds produced in the ascending cell walls), and that the closed cells are produced by ascent in the cell center and descent (thus cloud evaporation) in the cell walls.

Figures 1, 2, and 3 show that the cloudy regions are filled with many individual cloud elements. The direction of motion and the turbulence distribution about each element is not the cellular motion considered here. Rather, a slow, mesoscale circulation is proposed that tends to enhance and maintain the cloudiness in the ascent regions and to inhibit and evaporate clouds in the descent regions. Thus a slow, steady circulation is superimposed on the relatively fast, small-scale, vertical motion of the individual clouds; this is illustrated schematically in figure 4. Only the mesoscale circulation is believed to be the counterpart of the laboratory cells; the individual cloud motions are pertinent only insofar as they contribute to the turbulent mixing.

The influence of viscosity on circulation direction discussed in the foregoing pages is suggested to be applicable. Eddy viscosity produced by turbulent overturning can have significant vertical variation if the destabilizing effects change with altitude. Those effects are discussed in some detail below, but it suffices here to point out that large surface heating and superadiabatic lapse rates would produce large eddy viscosity (e.g., Craig [5]) near the surface, decreasing upward, even in the presence of clouds. Where the lower layers are only moderately warmed by the lower boundary, the overturning may increase upward because the cumulus cloud overturning, under those conditions, would exceed the surface turbulence.

The postulated circulation in open cells is also consistent with Stommel's proposed mechanism. In the open cells, descent would produce the greatest stability in the center, tending to inhibit turbulent mixing. Near the cell walls where the air is no longer subsiding, it would be less stable and greater turbulence would develop. Lowest horizontal speeds (near cell walls) would therefore be associated with greatest eddy viscosity, and the lowest viscosity would occur near cell centers with higher velocities.

With closed cells, however, application of Stommel's argument is not apparent, and the minimum friction condition, if applicable, must be due to other flow and stability effects. Notice that this does not detract from the analogy because theory has shown that a vertical gradient of viscosity may be sufficient to determine the direction of circulation.

A point critical to the validity of the proposed analogy concerns the generation and maintenance of thermal instability and its appropriate vertical distribution. It is proposed that the required

instability is produced by various combinations of the following processes:

- a. Sensible heat flux from the surface;
- b. Longwave radiation from the air and clouds, together with the opposing influence of direct absorption of shortwave radiation;
- c. Evaporation of cloud droplets into an overlying dry layer;
- d. Release of latent heat; that is, cumulus cloud formation by any means (turbulent mixing, convergence, differential advection).

The first three modify the vertical distribution of temperature and thus the stability. Heat loss from the layer top and/or heat gain near the bottom act to destabilize the layer, which if sufficiently perturbed, commences overturning. The effect of condensation on eddy mixing is somewhat different.

Cumulus formation adds heat, first at the condensation level then at successively higher levels as the cloud grows. But this temperature change does not affect the stability in the same manner as do those resulting from the other processes. Increasing the temperature at middle and upper levels is stabilizing when produced by processes a, b, or c, but when condensation adds heat to the upper portion of the layer, the effect is not stabilizing, rather overturning increases because of the onset of cumulus convection. Hence from the standpoint of eddy viscosity, heat added to the upper layers by condensation cannot be considered in the same way as the other temperature changes. This is not a serious complication because, as a first approximation, latent heat can be neglected insofar as it affects layer instability. This is not to say that cloud formation is unimportant to mesoscale cells; the point is that latent heat released in the upper part of the convective layer cannot be considered equivalent to an equal heat gain by, say, absorption of insolation. The latter tends to inhibit overturning whereas the former increases overturning. The intensity of turbulent mixing in clouds is not simply related to the amount of latent heat released, therefore its neglect may not be serious in considerations of eddy viscosity.

Latent heat might also be neglected from the standpoint of energy required to drive the mesoscale cells against stability and friction. Examination of the observations shown on figures 6 through 26 show that for the most part little or no precipitation is falling from the cells. If the primary energy were realized from latent heat, the condensed water would have to fall out. Lack of rain is strong evidence that there is little energy from this source.

Some order of magnitude estimates can be made for the first three destabilizing effects and this is done in order to determine if they are plausible primary factors. Because they operate at different levels in the convective layer, their relative magnitudes could produce vertical variations of instability, and presumably could cause the vertical variation of turbulent mixing on which this analogy depends.

Sensible heat flux from the surface, according to Petterssen [21] can be estimated by:

$$F = 4.7 \times 10^{-3} V(T_s - T_a) \quad (1)$$

where

$$F = \text{flux in cal. cm.}^{-2} \text{ min.}^{-1}$$

$$V = \text{surface wind speed in m. sec.}^{-1}$$

T_s, T_a = sea surface and air temperatures, respectively,
in degrees Celsius.

The data of Section II show a wide range of speeds and temperature differences. The extreme air-sea difference is shown in figure 5, where 25 knot winds are associated with temperature differences near 8°C. in open cells. The median value for the cases illustrated here is something over +2°C. in open cells and somewhat less than +1°C. in closed cells (Table 3). Some of the wind speeds are low, but the open cells are frequently observed in areas of 10 to 20 knots; closed cells appear to be associated with somewhat lower speeds.

For the purpose of an illustrative estimate, we use a speed of 8 m. sec.⁻¹ and a temperature difference of 2°C., which gives a sensible heat flux of 0.075 cal. cm.⁻² min.⁻¹. Inspection of Table 3 shows that this estimate could easily vary from case-to-case or area-to-area by a large factor.

Radiation heat loss by long waves and the direct absorption of insolation depend on the cloud and water vapor distribution both within the convective layer and above it, consequently it can be highly variable. Heating of clear air by insolation can be neglected, but significant amounts of short wave radiation are absorbed by clouds. Based on the data given by Fritz [7], a reasonable estimate for cloud layer heating is 0.11 cal. cm.⁻² min.⁻¹, where this is mean heating of the entire cloud layer, horizontally homogeneous, from, say, 950 mb. to 850 mb. If the sky were half covered, the heating for the layer would be approximately halved.*

* Clearly this is only a crude estimate but it would serve no purpose here to discuss differences brought about by drop size distribution, cloud-to-cloud radiation etc.

Long wave radiation was computed for the hypothetical sounding of figure 27 by use of a computation procedure described by Wark et al. [30]. The net long wave radiation, integrated for all zenith angles, is shown on the illustration at 50 mb. intervals for a cloudless sky and for the case of a black body cloud filling the layer 950 mb. to 850 mb. The cloud was assumed to be radiating upward at its 850 mb temperature and downward at its 950 mb. temperature, and the layer between cloud and surface to be in radiation equilibrium.

Net cooling of a layer is proportional to the flux divergence, and according to Kuhn and Suomi [13] the temperature change is

$$\frac{\partial T}{\partial t} = - \frac{g}{C_p} \frac{\Delta R_n}{\Delta P} \quad (2)$$

where ΔR_n is the flux divergence and the other symbols have their common definitions. Equation (2) is equivalent to

$$\Delta T (\text{ }^{\circ}\text{C}/\text{day}) = - 60 \Delta R_n \quad (3)$$

where the divergence is in units of cal. cm.⁻¹ min.⁻¹ (100 mb)⁻¹. Table 1 shows some computations of long wave cooling. For the purposes of approximate comparisons the flux divergence of the two layers under 5/10 sky cover is estimated to be the mean between clear and overcast conditions; a crude estimate, but adequate to illustrate the point. The line of Table 1, labeled "layer difference" cooling rate between cloudy and sub-cloud layers, represents the excess cooling of the upper layer; thus a larger number represents a greater destabilization. This shows that below the inversion (see fig. 27) the long wave cooling is only slightly different from top to bottom if the layer is cloudless, but the presence of a cloud deck produces intense destabilization. These estimates compare quite well with James' [10] computations of radiation loss from a stratocumulus deck. He also measured the turbulence at cloud top, thereby verifying the nighttime instability.

Evaporation from cloud tops is a heat sink at the upper boundary and thus a destabilizing influence. Data are not available to make any reasonable estimate of this effect but a crude guess at an upper limit will demonstrate that this particular component can be ignored. Many of the cases illustrated in Section II occurred in the subtropical Pacific where Riehl et al. [24] studied the trade wind layer. Their mean data, representative of our Pacific cases, is used for this upper limit estimate.

They showed that the thickness of the moist convective layer increased downstream, opposing subsidence of the mean flow, due to evaporation of overshooting cumulus tops into the overlying dry layer. We compute the mass of water that is transported through the top of the initial (upstream) moist layer and assign all of that transport to overshooting cloud tops. Clearly some of the vapor is transported by turbulent mixing of vapor, so the assumption of moisture flux

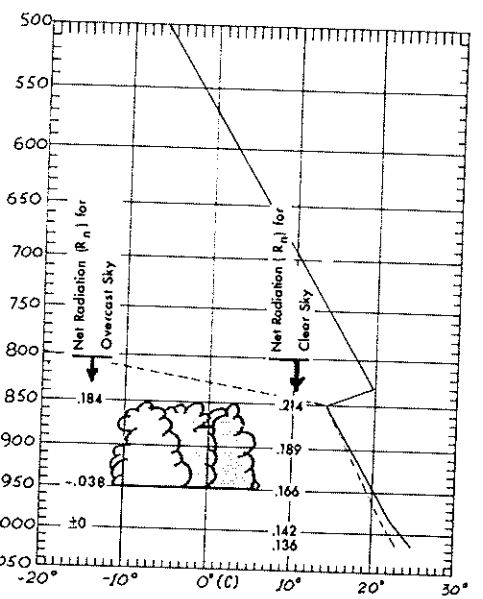


Figure 27. Hypothetical sounding and location of clouds for which net longwave radiation (R_n) (cal. cm.⁻² min.⁻¹) was computed, positive for outgoing, for two sky conditions.

TABLE 1. LONGWAVE FLUX DIVERGENCE AND COOLING FOR CLOUD AND SUBCLOUD LAYERS

Layer	<u>Flux Divg. (Cal. cm.⁻² min.⁻¹ layer⁻¹)</u>		<u>Cooling for 100 mb. Layer (°C. day⁻¹)</u>		
	Clear	Overcast	Clear	Overcast	5/10
1015 mb. to 950 mb.	.136-.166= -.030/65 mb. = -.046/100 mb.	+0	2.76°	±0	1.4°
950 mb. to 850 mb.	.166-.214= -.048/100 mb.	-.038-.184= -.222	2.88°	13.3°	8.1°
LAYER DIFFERENCE (Excess cooling in upper layer)12°	13.3°	6.7°	

entirely by droplets is a gross overestimate; the evaporation cooling based on this assumption is likewise a gross overestimate. The equation used to compute the evaporative cooling per unit area per unit time is,

$$E = \frac{\Delta Z \rho \Delta q L v}{2X} \quad (4)$$

where,

E = Evaporative cooling, cal. cm.⁻² min.⁻¹

ΔZ = Increased depth of moist layer = 1085 m.*

ρ = Air density at 950 mb. 10^{-3} gm.cm.⁻³

Δq = Increase in mixing ratio due to evaporation = 3 gm./kg.*

L = Heat of vaporization = 5.8×10^2 cal.gm.⁻¹

v = Mean wind speed = 6.2 m. sec.⁻¹ *

X = Length of trajectory = 2365 km.*

Substituting these values in (4) yields a heat loss of 0.015 cal. cm.⁻² min.⁻¹. If we assume this is distributed through a 50 mb. layer at the top of the moist layer it would produce a cooling of less than 2°C. per day; and for comparison later, this is equivalent to 1°C/day for a 100 mb. layer. Because this is a gross overestimate of the cooling that could be realistically produced, and because it is already smaller than the cooling caused by cloud radiation, we conclude that evaporative cooling is an insignificant destabilizing effect for mesoscale cells.

Table 2 shows that sensible heat flux from the surface and radiation balance of the cloud layer are probably primary mechanisms that maintain the instability, thus providing the circulation energy. Moreover, these two factors, one operating at the bottom of the convective layer, the other near its upper boundary, are both destabilizing and can be of the same order of magnitude. As a consequence the instability can increase upward or decrease upward, depending upon the relative magnitudes of these two factors.

* Data taken from Riehl et al. [24].

TABLE 2. SUMMARY OF DESTABILIZING TEMPERATURE CHANGES
(EXPRESSED IN TERMS OF 100-MB. LAYERS)

<u>Surface Heating</u> (For typical values $\Delta T = 2^{\circ}\text{C}$, wind speed = 8 m. sec. ⁻¹):		4.5°C./day
<u>Radiation</u> (Net of longwave plus shortwave):		
<u>Local Noon</u>	Clear Sky	0.1°C./day
	5/10 Clouds	3.4°C./day
	Overcast	6.7°C./day
<u>Low Sun</u>	Clear Sky	0.1°C./day
	5/10 Clouds	6.7°C./day
	Overcast	13.3°C./day
<u>Evaporation Cooling</u> For Mean Trade Wind Conditions:		$\ll 1.0^{\circ}\text{C}.$ /day
<u>Latent Heat</u> :		Nil

Layer instability can be induced by differential advection or by vertical stretching resulting from convergence. Neither of these effects appears to be credible in the cases shown here with low level inversions, but they might operate when deep layers are involved. Figures 6b, 8b, and 12b (Lerwick) show no low level inversion and it is possible that cold advection increasing with height or convergence may have been enhancing instability. The purpose here, however, is to examine the effects that appear to produce the smaller scale vertical variations of stability, and not the larger scale superimposed influences.

The results shown in Table 2 cannot be viewed as anything more than illustrative because, for example, the surface heat flux will not necessarily raise the temperature of the lowest 100 mb.* Likewise the radiation cooling, being a maximum in the top few meters of the cloud layer, will produce overturning and cooling through a layer whose thickness depends upon various characteristics of the cloud layer.* The relative magnitudes do reveal, however, which of the variables must be measured when we mount an experimental program.

One further observation may bear on the need for quasi-steady heating from the surface to produce open cells. Well-formed open cells are rarely observed over land, no doubt due to the disturbing influence of rough terrain on the weak circulation of these flat cells. Some continental areas, however, are no rougher than the ocean surface with 15 to 20 knot winds, but it appears that open cells form only under conditions that are short-lived on continents. A few cases of open cells were observed in cumuli and stratocumuli of cold air flowing over land well-soaked by earlier frontal rain. When there are puddles of surface water and saturated soil the specific heat is large, so the surface continues to be a steady heat source much like the ocean. When the surface dries it can cool quickly, and its temperature then follows closely the overlying air temperature.

The most clear-cut case occurred on 11 September 1964 when an arctic airmass moved over the Canadian province of Quebec. The frontal rain soaked the surface and a large area of open cells appeared 300 to 700 km. behind the frontal band.

Other open cell areas have been observed where the terrain is quite flat and very cold air moves over a warmer surface.

Diurnal and Irregular Changes

If the cell type is strongly influenced by changes in radiation and surface heating, diurnal as well as other time changes might be expected.

* Craig [5] reported on the depth of the surface layer in which intense heating produced superadiabatic lapse rates. In 105 cases all but two superadiabatic lapses were confined to layers less than 100 ft. deep.

For example see the turbulence measurements reported by James [10].

Assuming the proposed hypothesis to be valid, consider the following situation: mesoscale open cells observed during high sun exist because surface heating is destabilizing the sub-cloud layer more rapidly than radiation cooling is destabilizing the cloud layer. Suppose that the surface heating is barely adequate to maintain open cells. Because short wave cloud heating is counteracting long wave radiation, only modest surface heating is necessary during the day, but when the sun sets the situation changes. Radiation cooling can increase by a factor greater than two, so that destabilization of the cloud layer could then exceed the destabilization of the sub-cloud layer. The atmosphere has thus simulated Tippelskirch's results with sulfur and the cell type should reverse.

Irregular time changes of cell type might also occur as the air approaches equilibrium with the underlying water. While the air-sea temperature difference and wind speed are large the surface heating would dominate, but when the air is only a degree or so cooler than the surface, the two effects would become nearly equal. At this point the balance could be determined by secondary factors such as the humidity of the overlying middle and high atmosphere, the presence of a thin cirrus shield, or a small change of surface wind speed.

Inspection of a large number of cases, and allowing for the uncertainties in ship's observation accuracy, it is apparent that:

1. Open cells exist under conditions of both small and extreme surface heating. Comparison of figures 5 and 21 illustrate the range of heating with open cells.
2. Closed cells exist only with small surface heating. None of the figures show closed cells with a case of reliably-documented large surface heating, nor has any come to the writer's attention.
3. The surface-observed variables of air-sea temperature difference and wind speed apparently are related to cell type in a fashion that is consistent with the hypothesis, as shown in Table 3.

Data for Table 3, drawn entirely from Section II, shows a number which is proportional to surface heating (knots x °C), tabulated by class intervals versus cell type. Following the hypothesis, it is suggested that all negative values in Table 3 are in error and should be disregarded.* The data that produced negative heating estimates

* An unsuccessful attempt was made to improve the quality of $(T_s - T_a)$ by analyzing the two temperature fields independently. The results were even more mixed than the "uncorrected" temperatures, consequently the raw data were used for Table 3.

TABLE 3. FREQUENCY OF $V(T_s - T_a)$ [kt.-°C] BY CELL TYPE

$V(T_s - T_a)$ [kt.-Deg]	OPEN CELLS	CLOSED CELLS
> 100	3	
81 to 90	3	
71 to 80	1	
61 to 70	3	
51 to 60	1	
41 to 50	2	
31 to 40	3	
21 to 30	2 — Median	2
11 to 20	8	4
0 to 10	5	8 — Median
- 1 to - 10	0	0
-11 to - 20	(1)*	2
-21 to - 30	0	0
-31 to - 40	(2)*	0
-41 to - 50	(3)*	1

*SURFACE DATA WHICH PRODUCED $V(T_s - T_a) < 0$

	OPEN CELLS			CLOSED CELLS				
	$V(\text{kt.})$	$T(\text{°C.})$	$^{\circ}\text{F}$	From Fig. No.	$V(\text{kt.})$	$T(\text{°C.})$	$^{\circ}\text{F}$	From Fig. No.
(1)	20	-0.6,	-1.	7b	10	-1.1,	-2.	15b
	10	-1.1,	-2.	23b	20	-0.6,	-1.	17b
(2)			None			20	-1.7,	-3.
(3)	20	-2.2,	-4.	15b	None			

are listed in the second part of the table to enable the reader to identify the surface reports shown in Section II. Inspection of surrounding reports gives some support to the suggestion that they could be in error. The table shows that both cell types occur when $V(T_s - T_a) \leq 30$. According to equation (1) this figure of 30 knot-degrees corresponds to about $0.07 \text{ cal. cm.}^{-2} \text{ min.}^{-1}$ and a heating rate for a 100 mb. layer of 4°C. per day . Table 2 shows that the net cloud top cooling probably is of this same order (7°C/day at night; 3°C/day during daylight).

The results are therefore consistent with the hypothesis that cells may be of either type when the surface heating is nearly equal to the cloud top cooling. The evidence, while suggestive, is inconclusive because the results depend upon the thickness of the layer chosen for each computation. Also consistent with the hypothesis is the observation that if cells form, only open cells occur with intense heating.

The same considerations apply to expected diurnal changes of cell type. According to the hypothesis neither open cells in regions of intense surface heating nor closed cells should be changed by increased radiation cooling at night, but open cells in regions of small surface heating might change to closed cells at night.

The Nimbus high resolution infrared (HRIR) data were examined for evidence of diurnal changes, but with uncertain results. The principal uncertainty is due to the low resolution of HRIR displays compared to the photographs taken in the visible.* Not only is there a large size difference between television scan line and HRIR scan line, but also the contrast between cloud and sea surface is usually smaller in the infrared than in the visible because the cells are formed in bright but warm clouds.

No good case of diurnally reversing cell type was located; a result that is not surprising when we consider the relatively small areas and times in which this should occur (according to the proposed mechanism). In regions of moderate to intense surface heating the diurnal change of cloud top radiation cannot reverse the vertical variation of eddy turbulence, so vast areas of cold air intrusions over water should support open cells both day and night.

Closed cells that exist during the day should remain closed at night. In addition, if the proposed mechanism is valid, there should be a tendency for the closed cells to persist once they form during the night because the closed type appear to create a greater sky cover. The cloud deck, once formed produces a large radiation loss that may not be compensated during the following day. Consider

* Resolution of HRIR data has been examined by Widger, et al. [32]. They estimate 2 to 5 miles, depending on direction of scanning.

a near-equilibrium region of open cells where the surface flux was heating the sub-cloud layer 4°C./day while the cloud layer net cooling was but 3°C./day at high sun. During the night the cell type might change when the cloud net cooling exceeded 10°C./day , producing an increase of sky cover from say 4/10 to 8/10. During the next high sun the cloud net cooling may decrease to 7°C./day (See Table 2) but this still exceeds the 4°C./day surface heating so open cells could not reform.

Two pairs of subtropical patterns that exhibit some change are shown in figures 28 and 29. The half-day displacement is not known but is probably no more than 200 miles; the general area, not specific points, should be compared.

Figure 28 is a TIROS picture at 07 GMT and a Nimbus HRIR display about 13 hours later. In the earlier picture (right) the whole area 50° to 55° southeast of the 45th meridian shows open cells. In the left picture the area is much more cloud covered and could be closed cells.

Both pictures of figure 29 are from Nimbus. At about 0830 GMT the area from 28° to 34°S , centered on 58°E . is open, but on the right, an HRIR picture 11 hours later shows that the cloudiness had increased. Had the cells remained open, they were of ample size to be resolved by HRIR data. Unfortunately the closed cells, if they existed in these pairs, were not resolved, and the data illustrate only change of open cells but no direct evidence of closed cells.

In view of the rather special circumstances that must coexist to obtain pictures of cell type change, the failure to locate a clear example is not surprising, nor is it damaging to the hypothesis.

A transitional pattern of cellular convection might be expected if air moves into an environment which reverses the dominance of surface heating versus radiation cooling. Such a pattern is suggested in the Nimbus picture of figure 30. Along the top of the picture are open cells and along the bottom of the picture are closed cells.* Running diagonally across the center are a series of radial groups lying between the open and closed cells. This type of pattern has been photographed several times and is always associated with mesoscale convection, suggesting that it is a transitional pattern. Other examples may be seen in the "Picture of the Month" series of the Monthly Weather Review, January 1963, January 1965, and April 1965 (Vols. 91, 93).

* The apparent mismatch between the upper and lower pair is due to a slight scale change and the change of sensitivity of the Nimbus vidicon from top to bottom.

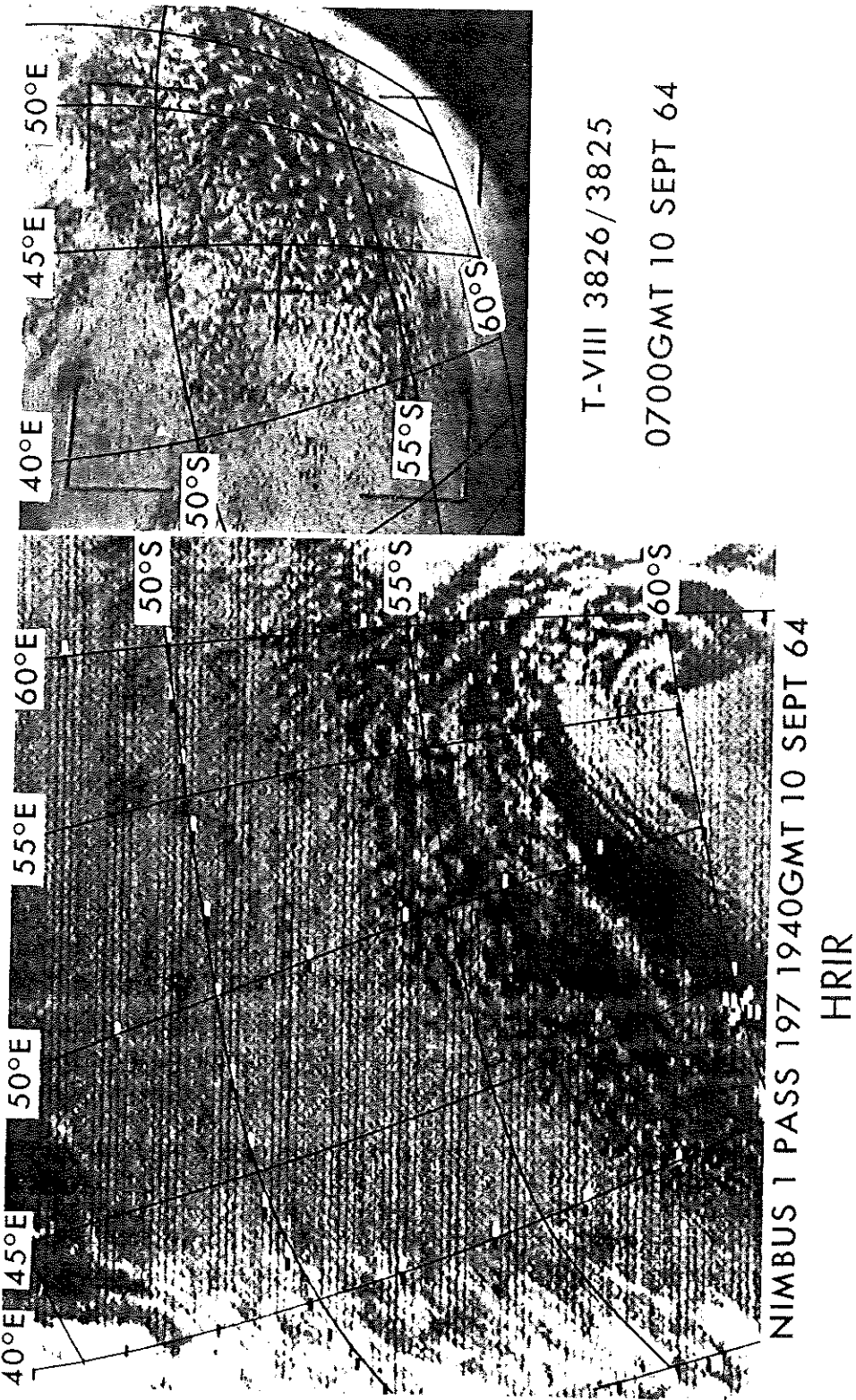


Figure 20. NIMBUS HRIR and TIROS VIII picture illustrating day to night difference of cellular clouds.

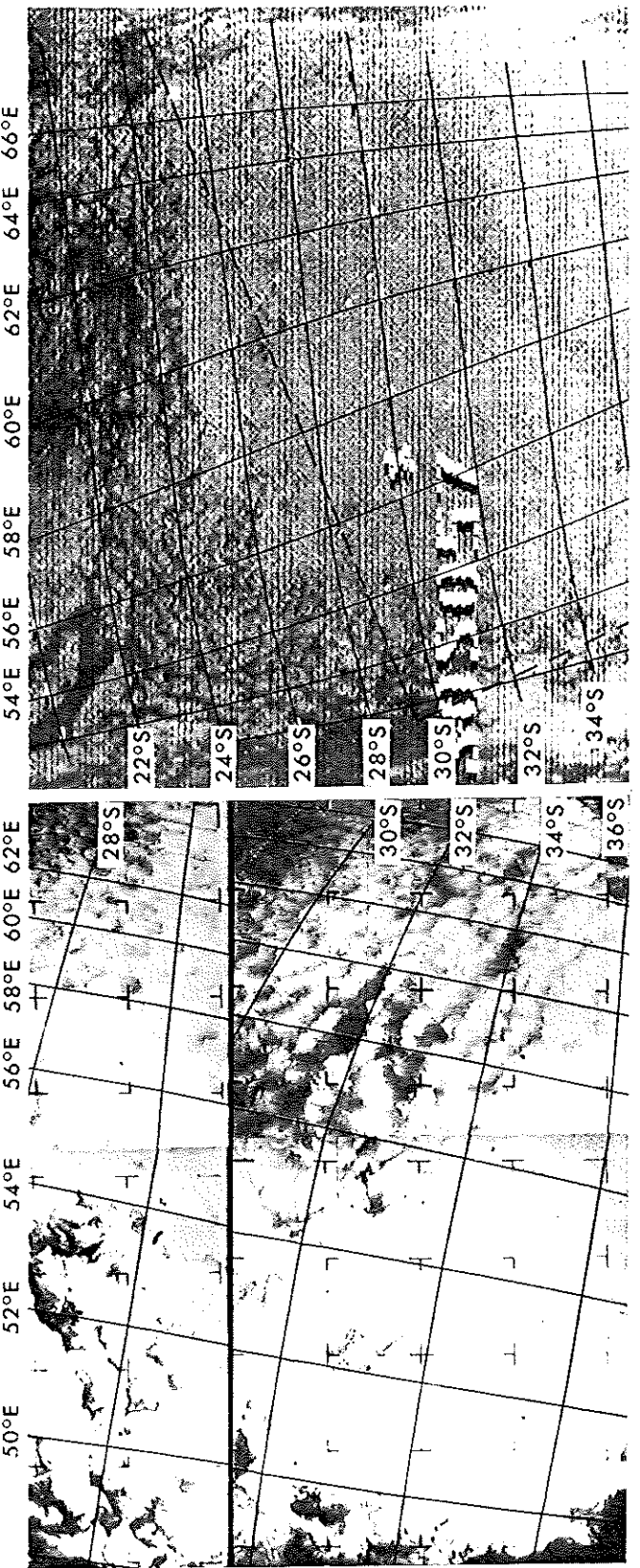


Figure 29. Nimbus HRIR and Advanced Vidicon Camera pictures illustrating day to night difference of cellular clouds. Broken line on right picture shows position of top and corner of left

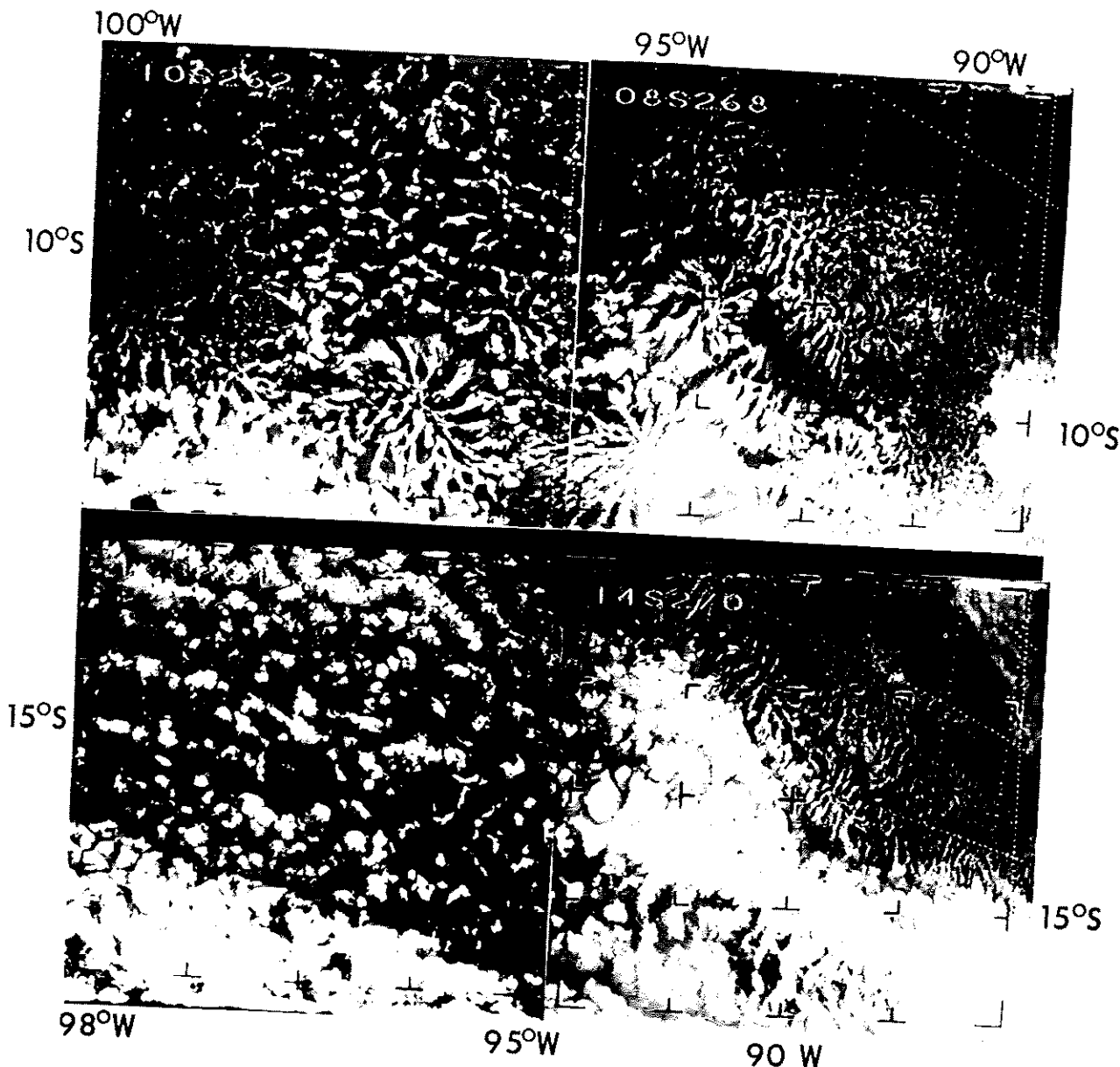


Figure 30. Nimbus picture of open cells (top) closed cells (bottom) and radial pattern that may be a transitional form.

These pictures were sent to Dr. Tippelskirch with the suggestion that they might be transitional patterns, and asking his opinion. He replied that when he obtained cell reversal in his experiments [30], he had observed a few ray-like forms that might have been their counterpart. 29

The illustrations in Section II indicate, however, that cells might change type without passing through the configuration seen in figure 30. For example figures 19 and 21 show a sharp boundary between cell types. The boundary changed orientation only slightly during this 24-hour period and moved downstream at about the wind speed. If the change of cell type were indeed produced by reversal of the heating-cooling dominance, the explanation for lack of a transitional pattern may be that those heating-cooling conditions were also moving with the general airflow. If true, cells of a given type would move very slowly through the boundary and quasi-steady state would be maintained, and thus no transitional pattern could form. No data are available to verify this speculation, but it suggests the type of measurements required.

Initial Instability, Shear, Cell Size and Rotation

Theory and experiment have indicated various properties of convection (other than direction of circulation) that might have counterparts in mesoscale cells. The heading of this subsection lists items that have been studied theoretically and in the laboratory. If the similarities between laboratory and atmosphere do not appear, it is instructive to examine the physics of the situation to search for an explanation. A tentative explanation, in turn, can be investigated in a field program.

The arrangement of ascending and descending columns of fluid that begin at the time of initial instability is not necessarily the cellular pattern we are considering here. Graham's experiments [9] demonstrated this, and he states, "If, then, we distinguish between the initial...motions...and the steady-state which ensues...the motion ...is in columns (originating at) the unstable surface. ...When conditions have become steady, polygons with descent in the centers... are formed."

Dassanayake [6] and Chandra [3] produced a mode of convection that set in at Rayleigh Numbers that were too low. Sutton [29] showed that this was due to instability in a thin layer near the heated boundary, and thus that the instability was not adequately represented by the temperature difference over the entire depth. Discussion of convective cells in the atmosphere must therefore take into consideration the possible difference between steady-state and initial instability.

The great extent of mesoscale cells over oceans suggests they are in quasi-steady state. But when cold air first flows off continents over warm water the onset of heating is abrupt and steady-state cannot

exist. It is of interest to study such situations to determine the period required to attain the conditions necessary for cells.

Unfortunately, shallow layers of fast-moving air have considerable vertical shear due to surface friction. Both theory and experiment have shown that three-dimensional cells can exist only in the absence of vertical shear. In the presence of shear, convection arranges itself into a two-dimensional pattern of rolls oriented along the shear vector.

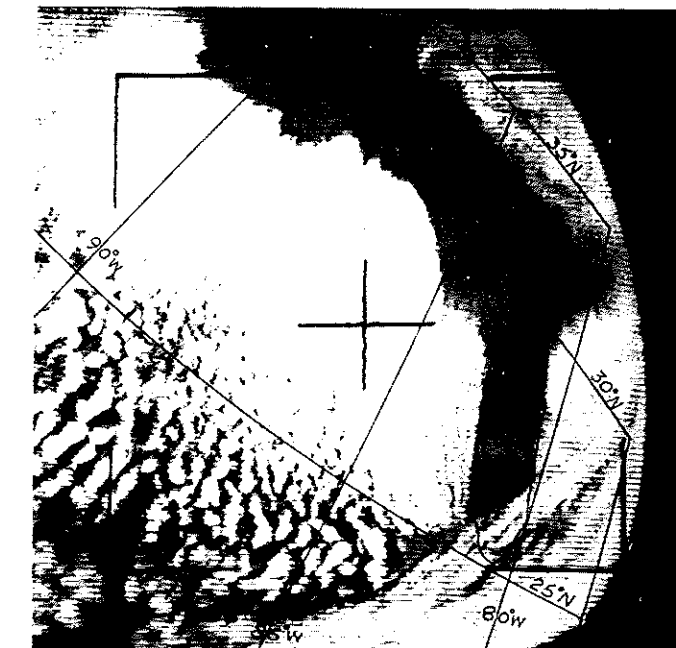
Brunt [2] summarized the laboratory results on the effect of shear. Woodcock [33] used soaring gulls as tracers and Kuettner [12] studied cloud rows to show a similar effect of shear in the atmosphere. But this straightforward effect of shear is vastly complicated by different scales of atmospheric convection, as can be seen by examining the patterns discussed by Malkus and Riehl [16].

Figures 31 and 32 are two examples of patterns frequently photographed when cold air flows from land across warm ocean. Immediately offshore the continental air is too dry to form clouds, but within a few hours' trajectory, flat cumuli appear beneath the inversion in the form of cloud lines oriented along the mean wind. Under these circumstances the shear vector would be expected nearly along the mean wind direction. Both figures show thin cloud lines oriented in this way. At the upwind edge of the pattern individual cloud lines are below the resolution limit of the television pictures, and thus the appearance is that of a uniform gray area. Further downwind the individual cloud lines can be distinguished.

Both the height of the mixed layer and the width of the cloud lines increase downwind, and the line-like character changes and mesoscale cells appear. On both figures a trajectory and a time have been computed from the surface data shown. In these cases 14 and 16 hours respectively, was required to develop the cellular pattern. Interpolation between the soundings of figure 31 indicates that the inversion height increased from 740 to 1220 meters during this time.

The following events are suggested by the data. In thin layers where the instability and shear are large, there form two-dimensional rolls whose spacing is proportional to the layer depth. When the layer reaches some critical depth, the vertical shear produced by surface friction becomes small enough* to permit three-dimensional cellular convection. Typical layer depth for this transition is somewhat in excess of one kilometer for intense surface heating and wind speeds in the 20 to 30 kt. range (compare these variables in the open cells of figure 5). Since the shear is a function of wind speed and surface heating, the critical layer depth should be smaller for less heating and lower wind speeds.

* Data currently available is inadequate to determine just what magnitude of vertical shear is "small enough." The winds observed with the cell cases in Section II show magnitudes of 0 to 4 kt. per 1000 ft. within the cloud layer and perhaps as large as 6 kt. per 1000 ft. across the cloud base.



T-X 3039/3038 1640GMT 30 JAN 66

Figure 31a. Lines of cumuli in shallow cold air over the warm Gulf of Mexico becoming cellular about 450 km. offshore.

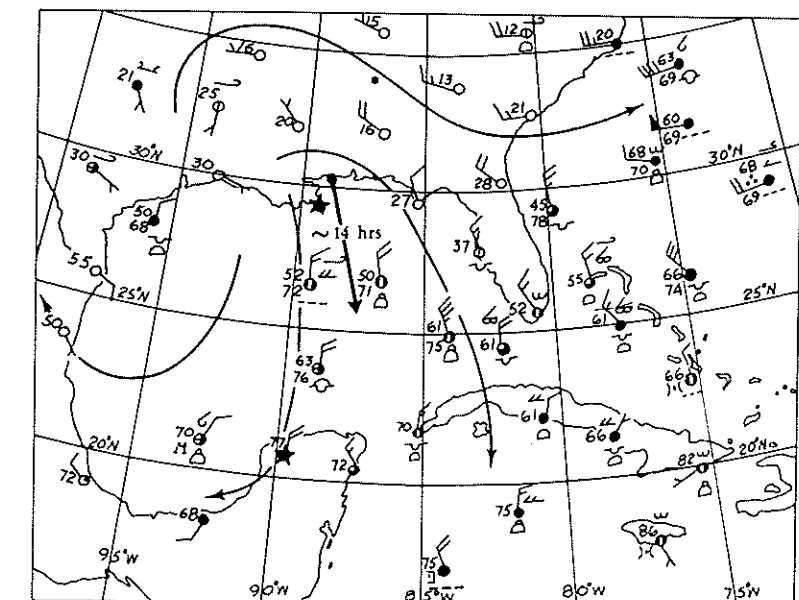


Figure 31b. Surface map and streamlines for 18 GMT January 30, 1966. Plotted digits are air and sea temperatures. Stars show radiosonde locations. Arrow indicates a 14-hour trajectory.

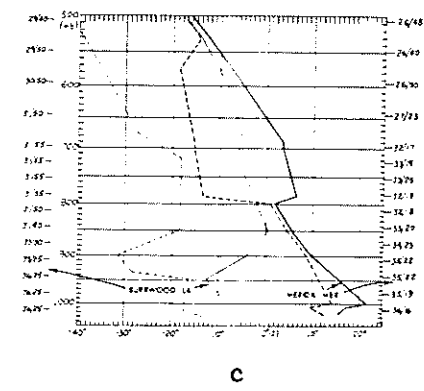


Figure 31c. Radiosondes for 12 GMT January 30, 1966. Wind directions to nearest 10 degrees/speed to nearest 5 knots.



T-X 3053/3052 1610GMT 31 JAN 66

Figure 32a. Lines of cumuli in shallow cold air becoming cellular about 400 km. offshore.

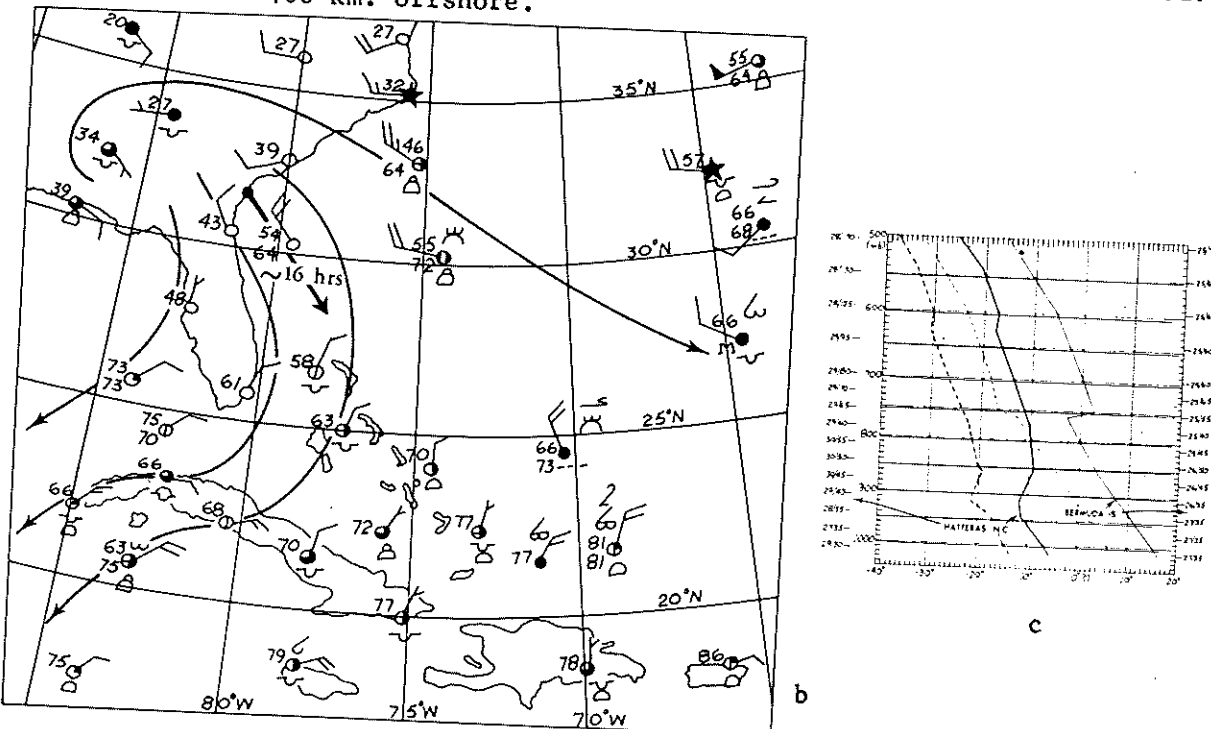


Figure 32b. Surface map and streamlines for 18 GMT January 31, 1966. Stars show radiosonde location. Plotted digits are air and sea temperatures. Arrow indicates a 16-hour trajectory.

Figure 32c. Radiosondes and winds, direction to nearest 10 degrees/speed to nearest 5 knots.

Tentative conclusions from the above discussion are (a) that quasi-steady state probably exists in the cellular patterns observed a day or more downstream from a sharp surface discontinuity and (b) that a quasi-steady state is needed to develop the pattern.

The size of cells can be estimated from satellite data and it is here that significant differences from laboratory cells appear. Theory, in reasonable agreement with laboratory results, yields diameter to depth ratios of approximately 3:1. But cells observed by satellite have diameter:depth ratios an order of magnitude greater. Fritz [8] shows a mean ratio of approximately 30:1 for a field of open cells in an Atlantic anticyclone. Avsec [1] cites a range of ratios from unity up to nearly six in various investigations by others, and he obtained a range from 1.74 to 3.85 in his own laboratory. Some of the variability he attributed to chance perturbations, but concludes there is a tendency for the cells to flatten as the depth increases. This result contrasts with the cases illustrated in Section II and discussed in connection with figure 34 below. In summary Avsec states that the cell dimensions should be proportional to the Rayleigh Number, but this relationship may not be applicable to the atmospheric cells for reasons discussed in Section IV.

Priestly [22] suggested that the flatness of mesoscale cells was due to the extreme anisotropy of the eddy coefficients. Subsequently Ray and Scorer investigated this mechanism theoretically, and some of the results were published by Ray [23]. The pertinent result is that flattening due to anisotropy was found, but with the following complications. The eddy transfers of both heat and momentum are involved. They are both anisotropic, but they are not necessarily equal nor equally anisotropic. The cell flattening was shown to be a function of two quantities, "m" and "n" that are measures of the anisotropy of the eddy transfer processes for heat and momentum.* Furthermore, diameter:depth (D/h) ratio was not uniquely determined by a single pair of values for m and n; instead, many different combinations are possible.

In summary, it is apparent that anisotropy of the eddy fluxes can produce cell flattening. It is reasonable that the ratio D/h can vary because the degree of anisotropy can change from case to case. There is suggestive evidence for this in figure 33.

Fritz [8] showed a positive correlation between cell diameter and layer depth. His graph is reproduced in figure 33 with the data

* Where K_x, K_y, K_z are eddy heat coefficients in familiar Cartesian notation, and ν_x, ν_y, ν_z are eddy viscosity coefficients: $K_x = K_y = mK_z$ and $\nu_x = \nu_y = n\nu_z$.

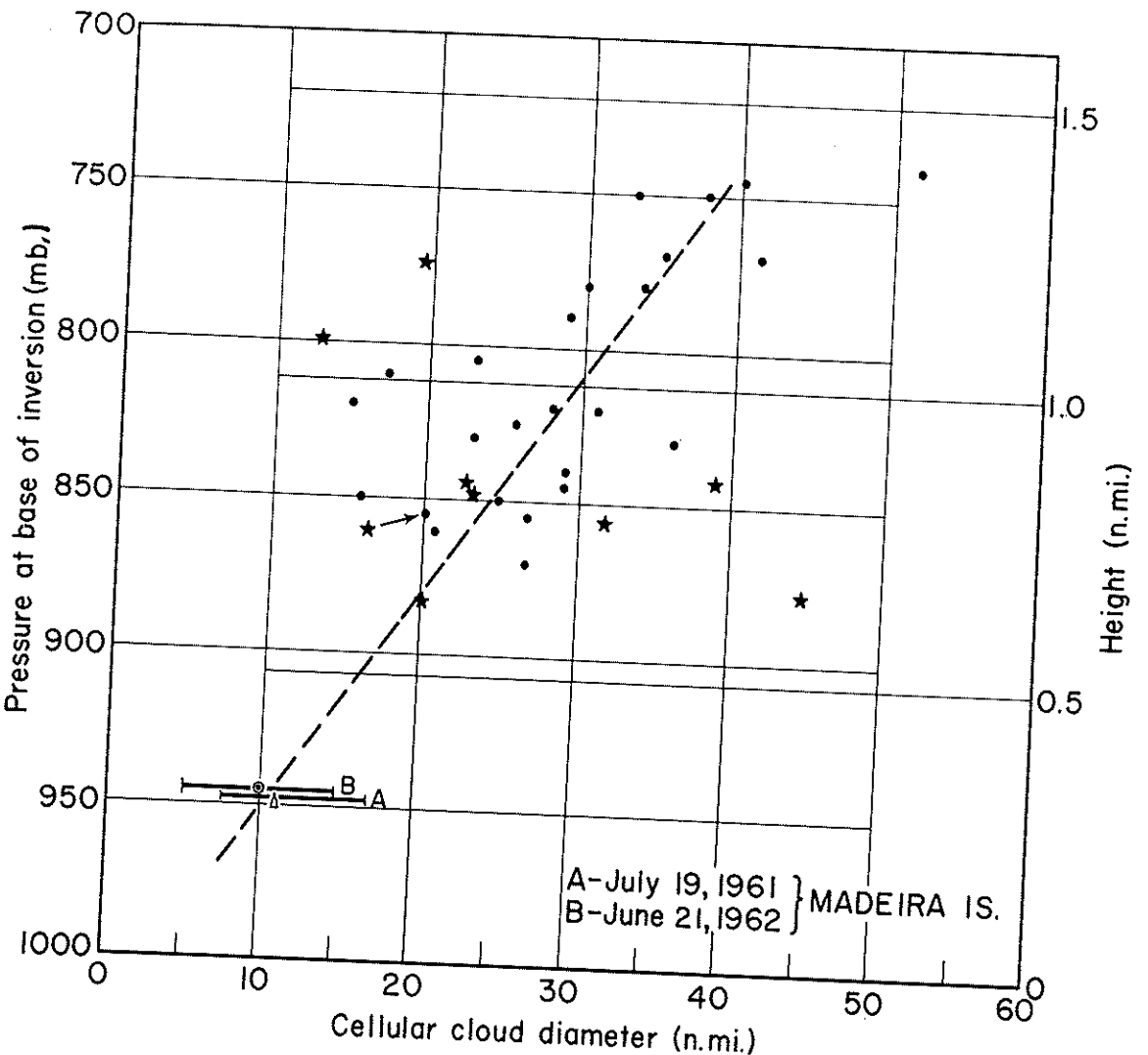


Figure 33. Cell diameter versus height of inversion. Original graph from Fritz [8]. Data points shown as stars are added from cases presented here.

from Table 4 added. Clearly the added data do not fit the original regression line. The original diagram is comprised of data from three different cases: two points were derived from small cells near Madeira Island and the remainder from a single Atlantic anti-cyclone (published earlier by Krueger and Fritz [11].) The data from Table 4, on the other hand, are from different locations, seasons, and synoptic situations. These contrasting results indicate that a given situation may produce cells with a small range of D/h ratios so that a plot of D versus h shows a positive relationship, but that different conditions yield different D/h values. A plausible reason is a change in the degree of eddy anisotropy under different synoptic situations.

One further work on cell size is pertinent: Kuo [14]. In the author's opinion this is a most significant contribution to the theory of mesoscale cells because he treats the real atmosphere with eddy processes. Kuo investigates two features, among others, that may be of overriding importance:

- (a) Effect of the cell scale on energy release processes.
- (b) Cell size as a function of the stability and the consequent ratio of ascent to descent areas.

A significant point of Kuo's theory is that, given a certain stability, the cell size that develops is of the scale that produces the most efficient liberation of convective energy.* Clearly this characteristic could be of great importance in the "calibration" of this convection, for it might turn out that the scale of observed cells reflects the rate of energy flux.

Relative to stability versus cell size, Kuo shows that the eddy viscosity might be estimated by measuring cell size. Because the magnitude and case-to-case variation of eddy viscosity is postulated (by the present writer) to be the pivotal characteristic of mesoscales, this promises an important experimental application (See Section IV).

Rotation theoretically can influence both stability and cell size. Chandrasekhar [4] and Nakagawa and Frenzen [17] have discussed four different effects of rotation that might influence cellular patterns:

- a. The stabilizing effect of rotation on convection.

* Kuo treats the release of latent instability as the energy source but it has already been shown that the cells under consideration are not so driven. The pertinence of Kuo's model is the concept of relating scale to the most efficient conversion of energy.

- b. The direction of circulation in cells, i.e., upward versus downward motion in the cell centers.
- c. The appearance of "over-stability" oscillations in place of convective instability.
- d. The size of the Bénard Cells.

The stabilizing effect is a function of the dimensionless quantity, the Taylor Number (T)

$$T = \frac{4\Omega^2 h^4}{\nu^2} \quad (5)$$

where

Ω = vertical component of the angular velocity

h = depth

ν = kinematic viscosity

Chandrasekhar [4] computed tables showing the increase of critical Rayleigh Number required for different Taylor Numbers. For convection bounded by one rigid and one free surface the critical Rayleigh Number is increased less than one percent for $T = 100$ and increased about 48 percent when $T = 2,000$.

The Taylor Number computed for reasonable values of atmospheric convection parameters* is less than unity. Rotation can be large in cyclones, but it would have to exceed the Coriolis parameter some hundreds of times to produce Taylor Numbers greater than the order of ten for shallow atmospheric layers. The inhibiting influence of rotation is therefore negligible compared to the effect of the various destabilizing forces already discussed.

The effect of rotation on direction of circulation within the cell was discussed by Nakagawa and Frenzen [17]. With high Taylor Numbers

* For example, for

$$\nu_{(eddy)} = 10^4 \text{ (a low estimate)}$$

$$\nu/\rho = 10^7 \text{ cm}^2 \text{ sec}^{-1}$$

$$\Omega = 5 \times 10^{-5} \text{ sec}^{-1}$$

$$h = 2 \times 10^5 \text{ cm.}$$

($T > 10^5$) the direction was apparently controlled by the choice of instability boundary. No experimental results have come to the author's attention that examine the circulation direction for very low Taylor Numbers. But by analogy with the results relating rotation and stability, it is probable that effects other than rotation determine the circulation direction.

Overstability oscillations in place of cellular convection are also of concern with high Taylor Numbers. Chandrasekhar [4] emphasized the importance of "overstable" oscillations in the atmosphere, because if overturning of the fluid first assumed this mode the pattern might be different from convection. Overstability would produce wave oscillations of increasing amplitude; presumably these would appear as wave clouds rather than cells. According to Chandrasekhar this mode of oscillation is possible if $H/\nu > 1.48$. Where eddy coefficients are involved it is possible that this value is commonly exceeded. However, overstability becomes a possibility only when the Taylor Number is large (perhaps $T \approx 10^3$). It is concluded, therefore, that rotation is not sufficient, in the cases we discuss here, to induce overstable oscillations.

Cell size is influenced by rotation according to Nakagawa and Frenzen [17], the diameter:depth ratio being inversely proportional to the angular velocity. Mesoscale cells show considerable size variation, so the data can be examined for this effect. A total of nine cell groups are available from the cases of Section II, for only the cells photographed in areas of soundings can be used. Table 4 lists the pertinent variables, and figure 34-a is a plot of the ratio D/h against angular velocity, Ω . The latter was computed from the surface streamlines, as follows:

$$\Omega = \frac{f}{2} + \frac{c}{R}, \quad (7)$$

where

f = Coriolis parameter

c = Surface wind speed

R = Radius of surface streamline curvature (anticyclonic curvature counted negative)

The diameters in most cell groups were recorded in terms of the smallest, the largest and the median; the graph shows a "+" at the ratio corresponding to the median diameter on the line representing the entire range.

An inverse relation between size and angular velocity is suggested but the sample is small. There is the possibility that the relation

TABLE 4. DATA FOR PLOT OF D/h VERSUS Ω AND h

From Fig. No.	Type of flow: C = Cyclonic A = Anticyclonic and Cell Type	Cell Diameter (D) min.-median-max D h	D/h min. med. max.	$\epsilon/2$ $\times 10^4$ sec. ⁻¹	Ω $\times 10^4$ sec. ⁻¹
5	Straight-Open	18-35-58	2.24	.489	.489
11	C-Open	20-25	1.94	.631	.801
11	A-Open	35-42-55	1.55	.597	.557
17	A-Open	33-43-74	1.48	.419	.350
17	A-Closed	44-82-124	1.20	.419	.283
19	A-Closed	37-59-85	1.42	.365	.143
21	A-Open	~ 37	1.15	.365	.275
23	A-Open	46-72-98	1.56	.365	.317
25	A-Open	20-37-74	1.43	.365	.359

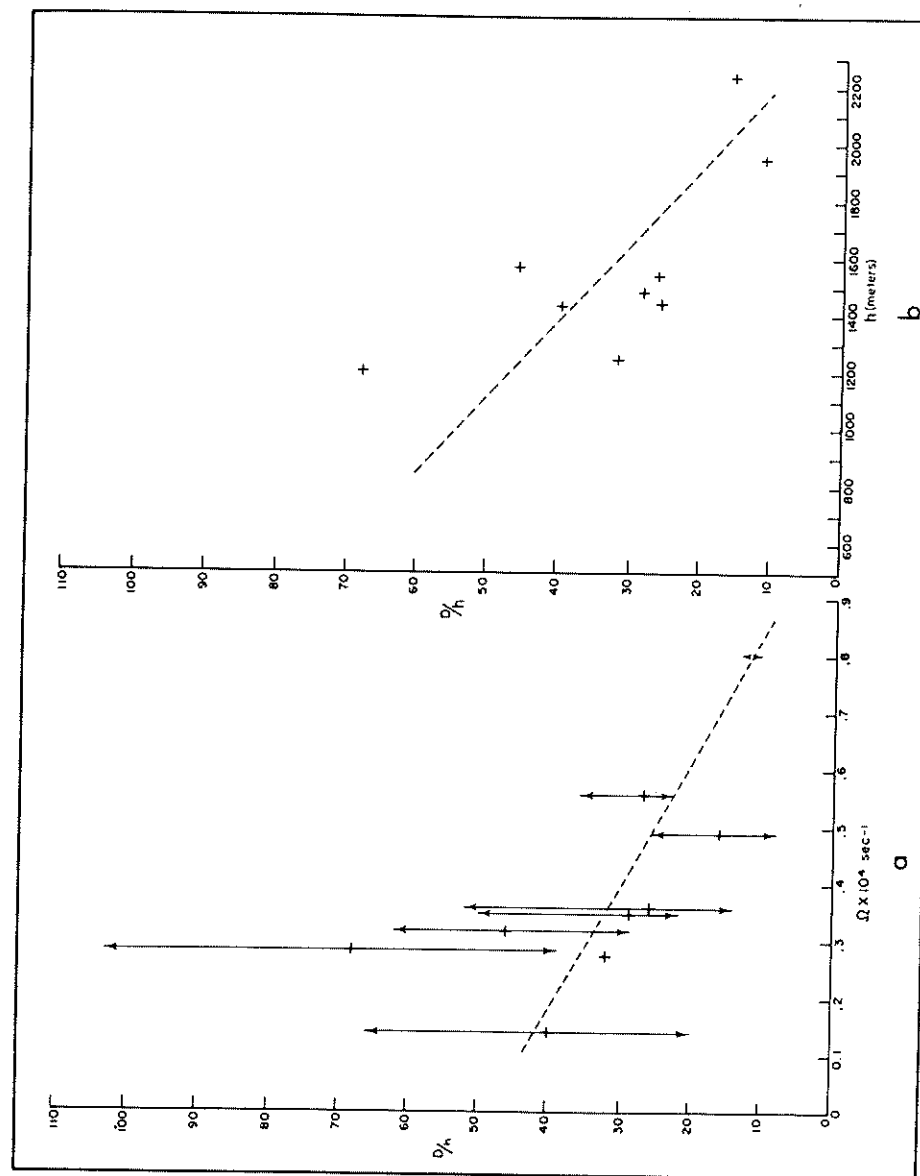


Figure 34a.

Plot of ratio diameter to depth (D/h) versus absolute angular speed (Ω). Heavy + is value of ratio for median D, arrows indicate ratio for entire range of diameters.

Figure 34b. Plot of ratio D/h (for median diameter) versus cell depth (h), ordinate same as above, abscissa cell depth (h).

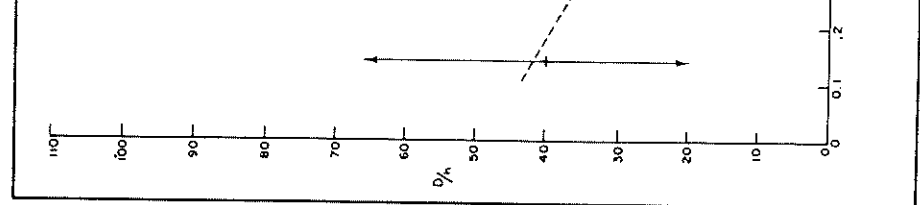


Figure 34b.

is only apparent, and is due to the chance correlation with some other parameter, such as layer depth. The graph of figure 34b is consistent with such an explanation, for the relation between D/h and h is somewhat better than the relation between D/h and angular speed.

Summarizing the effects of rotation on cells, it appears that rotation rates are too small to be significant in the shallow layers characteristic of cellular patterns. Data presented here are not sufficient to demonstrate this conclusion, but are consistent with it.

IV. SUGGESTIONS FOR FUTURE WORK

The phenomenon of mesoscale convection poses a difficult problem to both theoretical and experimental investigators. Theoretical models, it would appear from the evidence presented here, must incorporate diabatic energy sources other than the latent instability of moist air or the release of baroclinic instability. The problem seems to be analogous to the laboratory convection mechanism treated extensively in the literature, but an important factor in the atmospheric case may be the variable, anisotropic nature of eddy transfer processes.

Kuo's [14] approach may point the way because he relates scale to the magnitude of the eddy coefficients. Moreover, he incorporates a concept that is intuitively very attractive: the connection between scale of circulation and a maximized energy conversion mechanism.

The challenge that faces theoreticians is to construct models to simulate the real atmosphere by incorporating the true nature of atmospheric eddy exchange processes. Furthermore the evidence suggests that the diabatic energy source is surface heating and long wave cooling, although only the former may be adequate in some cases. Therefore, the minimal theoretical model must incorporate at least an energy source by strong surface heating and anisotropic eddy transfers of heat and momentum.

Experimental work will certainly be an important part of future investigations, but the experimenter must move out of the laboratory and into the atmosphere. The crux of the problem is apparently the complex role of eddy processes. It follows that real progress may depend on the success of making detailed measurement of heat fluxes, turbulent processes and radiation effects in fields of cells over the oceans. It is unlikely that measurements made over land and in different mesoscale regimes can be applied to the cellular regime.

A carefully designed field program is required to provide data applicable to this problem, but some aspects of the hypothesis might be checked by simple observations if they are made on the proper scale. An aircraft surveillance of cellular groups in regions of small heating could verify or disprove the diurnal changes of cell type. Coordinated

by satellite data, aircraft could also examine the transitional patterns and the sharp boundary regions between opposite cell types to test the suggestions concerning these changes of mesoscale regime. But a sophisticated program is necessary to obtain definitive data. Foremost among required measurements are those that can be used to evaluate the variable eddy coefficients and those that measure the destabilizing energy sources.

Eddy viscosity is a function of the vigor of eddy turbulence and vertical wind shear. The viscosity term in the Navier-Stokes equations is frequently written

$$\frac{1}{\rho} \frac{\partial}{\partial z} (\bar{T}_{zy}) \quad \text{or} \quad \frac{1}{\rho} \frac{\partial}{\partial z} (\nu_e \frac{\partial v}{\partial z})$$

because $\bar{T}_{zy} = -\rho \bar{v}' \bar{w}'$ then, $\bar{v}' \bar{w}' = \nu_e \frac{\partial v}{\partial z}$

where ν_e is eddy viscosity and the other terms have their conventional definition. Measurement of $\bar{v}' \bar{w}'$, for example with aircraft accelerometers, together with vertical shear, would provide estimates of ν_e . Although this quantity is a function of both shear and turbulence, it is fairly insensitive to roughness but very sensitive to vertical shear, according to Panofsky and Press [19]. This indicates that a field program to measure eddy viscosity in cells must insure the accurate sensing of shear over fairly small height increments.

Direct measurement of the destabilizing effect of heating and cooling must be made in order to study the cells' energy source, but additional insight might be obtained from the other parameters that influence stability. Rayleigh's well known criterion for the onset of convection is that the quantity (Ra) exceed a critical value, where

$$Ra = \frac{g \alpha \Delta T h^3}{K \nu} ; \text{ its expression for a compressible gas is}$$

$$Ra = \frac{g(\gamma - \delta)}{T(K\nu)} h^4 \quad (6)$$

where γ and δ refer to the dry adiabatic and actual lapse rates in the compressible fluid and

g = acceleration of gravity

α = coefficient of thermal expansion

ΔT = temperature difference from top to bottom of a fluid

K, ν = coefficients of thermal conductivity and viscosity, respectively

h = depth of fluid

The quantities in the denominator of (6) are the eddy coefficients, for it is well known that viscosity and thermal conductivity by molecular processes is many orders of magnitude smaller.

Introduction of eddy coefficients, unfortunately, renders the Rayleigh criterion less useful for atmospheric experimental work because they are highly variable. Even if the eddy coefficients were constant and known, the Rayleigh Number would be of limited use because it depends so critically upon the difference between the actual and the adiabatic lapse rates. Changes in the Rayleigh Number from a fraction of the critical value to many times that value can be produced by differences too small to be measured by radiosonde or aircraft sensors. A further difficulty is introduced whenever condensation occurs because buoyancy is added and the moist, not the dry, adiabatic rate should be involved in the Rayleigh Number for that part of the fluid.

Nevertheless the basic concept of the Rayleigh Number is applicable. The lapse rate difference ($\Gamma - \gamma$) represents the buoyancy forces. Overturning is resisted by the viscosity of the fluid and by its thermal conductivity. Viscous drag resists overturning and in addition, if the thermal conductivity is high, the lowest layers cannot become sufficiently buoyant to become unstable. Clearly these same opposing forces operate in the atmosphere. It is futile to attempt to evaluate the Rayleigh Number directly, but we can draw some information from the concept as follows.

The existence of mesoscale cells is evidence that a supercritical Rayleigh Number is being maintained for that particular scale of convection. Scale considerations are crucial because the quantities involved must pertain to the entire layer under consideration. (See Sutton's results in [28]). When cold air first flows over a warm ocean the lowest few hundred meters are very unstable, so at the scale of individual thermals the Rayleigh Number is supercritical. But at the scale of a deeper cold layer the Rayleigh Number may be subcritical. It follows that depth of the convective layer (for the scale of convection being studied) is critical since it enters to the fourth power. The product ($K\zeta$) is also a function of the scale because enhanced turbulence increases its magnitude. Therefore the increase of small-scale convection is stabilizing for the larger mesoscale overturning.

Existence of mesoscale cells, and the implied existence of a supercritical Rayleigh Number for the mesoscale, are evidence of an adjustment between (h^4) and ($K\zeta$) appropriate to a supercritical Rayleigh Number. Therefore accurate measurement of depth yields some information about ($K\zeta$), and if ζ were evaluated independently, also information about K .

V. SUMMARY OF CELL CHARACTERISTICS AND CONCLUSIONS

The data presented here demonstrate the existence of mesoscale cells and their prevalence over oceans. Only a few of the cell characteristics are definitively observed from available data, a few more characteristics are highly likely, but some must be considered hypothetical and tentative. In order to develop the author's hypothesis, experimental and theoretical results have been described as they seemed to apply to various observations of mesoscale cells. Consequently Section III is a blend of observations, experiments, theory and inference.

The observed mesoscale features are:

1. Mesoscale cells form in fields of cumuli or stratocumuli when the air is heated by the underlying surface. Characteristic cell diameters range from about 10 to 100 km. with the median size about 50 km. The diameter:depth ratios range from approximately 10:1 to 100:1 with a median ratio about 30:1.
2. Mesoscale cells are frequently confined to a shallow surface layer by a strong inversion. Where cells exist in a layer with no inversion, there is some evidence that the convective layer is limited instead by dry air entrainment.
3. Cells composed of cloudless centers and walls of clouds (viz. open cells) form in conditions of moderate to intense surface heating. Cells composed of cloud-filled centers and (nearly) cloudless walls (vis. closed cells) form in conditions of weak to moderate surface heating.

The mesoscale features that are strongly implied by available data are:

1. Cell formation requires quasi-steady state heating and negligible vertical wind shear.
2. The diameter:depth ratio varies from one (unspecified) synoptic situation to another.
3. Open cells are cloudless in their centers because of downward motion in cell center and upward in the walls. Closed cells have the opposite circulation.
4. The energy sources that drive the mesoscale cell circulation against static stability and friction are diabatic heating at the earth's surface and radiation cooling from cloud tops. Evaporation of cloud tops, release of latent instability, and the enhancement of instability by differential advection or convergence are all less important, secondary effects.

5. Rotation of the atmosphere about the local vertical has no appreciable effect on the mesoscale cells.

The inferred cell characteristics and the features that exist if the proposed hypothesis is valid are:

1. Mesoscale cells develop for the same reasons and in response to the same mechanism as Bénard cells in the laboratory, that is, eddy conduction of heat is insufficient to prevent the lower or upper (or both) portion of a stratum from becoming excessively unstable, eddy viscous forces are overcome, and cellular circulation begins. (In the laboratory molecular heat conduction and viscosity are the counterparts of eddy mechanisms of the atmosphere.)
2. The directions of circulation in cells which produce the open or closed cell type is determined by the vertical increase or decrease of eddy viscosity. This variation is determined by the relative magnitudes of turbulent overturning in the sub-cloud layer vis-a-vis the cloud layer. (In the laboratory the vertical variation of viscosity is determined by the vertical temperature distribution.)
3. The diameter:depth ratio of the atmospheric cells is controlled by the degree of anisotropy of the eddy viscosity and eddy heat conduction. The degree of anisotropy is different in different synoptic situations. The ratio is about an order of magnitude greater than for laboratory cells because molecular viscosity, by contrast, is isotropic.
4. Transitional patterns quite distinct from open or closed cells form if a given cell type is advected rapidly into an environment that tends to produce the opposite cell type.

In conclusion it is suggested that mesoscale convection is important in the air-sea interaction problem, both because it may represent a scale that makes a significant contribution to eddy exchange processes and because it may be a sensitive indicator of magnitude and distribution of eddy exchange coefficients. The author submits that this is, therefore, a significant problem for research.

The hypothesis proposed as explanation of the various inferred characteristics is speculative, but it can serve as a focus for investigations. If measurements appropriate to the hypothesis are made, it is probable that we will develop a fuller understanding of the phenomenon even if the hypothesis turns out to be invalid.

ACKNOWLEDGMENTS

Many of the staff of the Meteorological Satellite Laboratory contributed significantly to this study by collecting and plotting data, gridding pictures, and producing illustrations. In particular the author acknowledges the improvement in the manuscript that resulted from the critical reading by Dr. E. P. McClain and Mr. Arthur Krueger.

Valuable discussions with Mr. Arthur Krueger and Dr. Sigmund Fritz contributed to this study. The bibliography shows that they are the joint authors of the first publication dealing with mesoscale cellular patterns, and their continued interest in the subject has aided the present work.

REFERENCES

1. D. Avsec, "Thermoconvective Eddies in Air-Application to Meteorology," Scientific and Technical Publications of the Air Ministry Works of the Institute of Fluid Mechanics at Paris, No. 155, 1939, 253 pp. (Translated by Carl A. Ronne).
2. D. Brunt, "Experimental Cloud Formation," Compendium of Meteorology, Thomas F. Malone, Editor, Amer. Met. Soc., Boston, Mass., 1951, pp. 1255-1262.
3. K. Chandra, "Instability of Fluids Heated from Below," Proceedings Royal Society, (A), 1938, pp. 231-242.
4. S. Chandrasekhar, "Thermal Convection," Daedalus, vol. 86, No. 4, 1957, pp. 324-339.
5. R. A. Craig, "Observations of Vertical Temperature and Humidity Distributions in the Convective Layer Above the Sea Surface," Annals of the New York Academy of Sciences, vol. 48, Sept. 1947, pp. 738-788.
6. D. T. E. Dassanayake, "Study of Some Special Cases of Instability of Fluid Layers, Particularly of Such Cases as Have Applications in the Atmosphere," Unpublished Ph.D. Thesis, University of London, 1937.
7. S. Fritz, "Solar Radiant Energy and Its Modification by the Earth and Its Atmosphere," Compendium of Meteorology, American Meteorology Society, Boston, Mass., 1951, pp. 13-33.
8. S. Fritz, "Local Circulations," an unpublished paper to appear in Proceedings of the Workshop on the Use of Satellite Data in Meteorological Research, National Center for Atmospheric Research, Boulder, Colo., Aug. 1965.
9. A. M. Graham, "Shear Patterns in an Unstable Layer of Air," Philosophical Transactions Royal Society, London, 232 A, 1933, pp. 285-296.
10. D. G. James, "Observations from aircraft of temperatures and humidities near stratocumulus clouds," Quarterly Journal of the Royal Meteorological Society, 1958, vol. 85, No. 364, pp. 120-130.
11. A. F. Krueger and S. Fritz, "Cellular Cloud Patterns Revealed by TIROS I," Tellus, vol. 13, No. 1, 1961, pp. 1-7.
12. J. Kuettner, "The Band Structure of the Atmosphere," Tellus, vol. 11, No. 3, 1959, pp. 267-294.
13. P. M. Kuhn and V. E. Suomi, "Infrared Radiometer Soundings on a Synoptic Scale," Journal of Geophysical Research, vol. 65, No. 11, 1960, pp. 3669-3677.
14. H. L. Kuo, "Further Studies of the Properties of Cellular Convection in a Conditionally Unstable Atmosphere," Tellus, vol. 17, No. 4, 1965, pp. 413-433.
15. J. S. Malkus, "Recent Advances in the Study of Convective Clouds and their Interaction with the Environment," Tellus, vol. 4, No. 2, 1952, pp. 71-87.
16. J. S. Malkus and H. Riehl, Cloud Structure and Distributions Over the Tropical Pacific Ocean, University of California Press, Los Angeles, Calif., 1964, 229 pp.
17. Y. Nakagawa and P. Frenzen, "A Theoretical and Experimental Study of Cellular Convection in Rotating Fluids," Tellus, vol. 7, No. 1, 1955, pp. 1-21.
18. E. Palm, "On the Tendency Towards Hexagonal Cells in Steady Convection," Journal of Fluid Mechanics, vol. 8, Part 2, 1960, pp. 183-192.
19. H. Panofsky and H. Press, "Atmospheric Turbulence," Progress in Aeronautical Sciences, Pergamon Press, New York City, 1962, pp. 179-232.
20. A. Pellew and R. V. Southwell, "On Maintained Convective Motion in a Fluid Heated from Below," Proceedings Royal Society, (A) 176, 1940, pp. 312-343.
21. S. Petterssen, D. L. Bradbury, and K. Pedersen, "Heat Exchange and Cyclone Development of the North Atlantic Ocean," Final Report to Air Force Cambridge Research Laboratories, Contract No. AF 19(604)-7230, Project No. 86410, 1960-1963, pp. A1-76.
22. C. H. B. Priestley, "Width-Height Ratio of Large Convection Cells," Tellus, vol. 14, No. 1, 1962, pp. 123-124.
23. D. Ray, "Cellular Convection with Nonisotropic Eddys," Tellus, vol. 17, No. 4, 1965, pp. 434-439.
24. H. Riehl, T. C. Yeh, J. S. Malkus, and N. E. La Seur, "The North-East Trade of the Pacific Ocean," Quarterly Journal of the Royal Meteorological Society, vol. 77, No. 334, 1951, pp. 598-626.

25. B. Saltzman, Editor, Selected Papers on the Theory of Thermal Convection with Special Application to the Earth's Planetary Atmosphere, Dover Publications, Inc., New York, N.Y., 461 pp.
26. L. A. Segel and J. T. Stuart, "On the Question of the Preferred Mode in Cellular Thermal Convection," Journal of Fluid Mechanics, vol. 13, June 1962, pp. 289-306.
27. H. Stommel, "A Summary of the Theory of Convection Cells," Annals of the New York Academy of Sciences, vol. 48, Sept. 1947, pp. 715-726.
28. O. G. Sutton, "On the Stability of a Fluid Heated from Below," Proceedings Royal Society, (A) 204, 1950, pp. 297-309.
29. H. V. Tippelskirch, "Über Konvektionzellen, Insbesondere Im Flüssigen Schwefel," Beiträge Zur Physik Der Atmosphäre, Bd. 29, 1956, pp. 37-54.
30. D. Q. Wark, J. Alishouse, and G. Yamamoto, "Variation of the Infrared Spectral Radiance Near the Limb of the Earth," Applied Optics, Vol. 3, No. 2, 1964, pp. 221-227.
31. W. K. Widger, Jr., J. C. Barnes, E. S. Merritt, and R. B. Smith, "Meteorological Interpretation of Nimbus High Resolution Infrared (HRIR) Data," Report by Allied Research Associates, Inc., on NASA Contract NASA5-9554, Concord, Mass., Jan. 1966, 150 pp.
32. A. H. Woodcock, "Soaring Over the Open Sea," The Scientific Monthly, vol. 55, 1952, pp. 226-232.
33. E. Zipser, and N. E. LaSeur, "The Distribution and Depth of Convective Clouds Over the Tropical Atlantic Ocean, Determined from Meteorological Satellite and Other Data," Final Report to U. S. Weather Bureau WB Grant 36, December 1965, 96 pp.

- Number
- *19. An Investigation of Meteorological Satellite Characteristics for Continuous Earth Coverage, T. I. Gray, Jr., and S. F. Singer, (July 1963) PB 163745 \$4.60
 - 20. Conference on Satellite Ice Studies, M. D. Baliles and H. Neiss, (Ed.), (June 1963) PB 163746 \$9.10
 - 21. Calculations of the Earth's Spectral Radiance for Large Zenith Angles, D. Q. Wark, J. Alishouse, and G. Yamamoto, (October 1963) PB 167176 \$3.00
 - 22. Spectral Reflectance Photography of Earth from Mercury Spacecraft MA-8, S. D. Soules, (November 1963) PB 167177 \$2.00
 - 23. The Use of Satellite Cloud Photographs in Numerical Weather Prediction, M. A. Ruzecki, (December 1963) AD 423269 \$2.60
 - *24. TIROS Cloud Pattern Morphology of Some Mid-Latitude Weather Systems, H. J. Brodrick, Jr., (January 1964)
 - 25. Infrared Photography of the Earth from Mercury Spacecraft MA-9, S. Soules, (in printing)
 - 26. Meteorological Products from Digitized Satellite Vidicon Cloud Pictures, C. L. Bristor and W. M. Callicott, (March 1964) AD 600078 \$1.25
 - 27. Number reserved for future report
 - 28. Automatic Processing of Nimbus Infrared Radiometer Data, G. E. Martin and L. Rubin, (July 1964) PB 166590 \$2.00
 - 29. Tropospheric Conditions over the Tropical Atlantic as Observed by Two TIROS Satellites and Research Aircraft During 22 September 1962, H. M. Johnson and R. W. Fett, PB 167178 \$4.00
 - 30. Lowlight Coverage from Polar and Sun-Synchronous Orbits, R. L. Pyle, (April 1964) AD 600970 \$.75
 - 31. Specular Spectral Reflectance of Paints from 0.4 to 40.0 Microns, W. Y. Ramsey, (April 1964) PB 167179 \$2.00
 - 32. TIROS Photographs and Mosaic Sequences of Tropical Cyclones in the Western Pacific During 1962, R. W. Fett, (July 1964) AD 608095 \$5.00
 - 33. Wind Speeds from TIROS Pictures of Storms in the Tropics, A. Timchalk, L. F. Hubert, and S. Fritz, (February 1965) PB 167180 \$2.00
 - 34. An Investigation of Degradation Errors in TIROS IV Scanning Radiometer Data and the Determination of Correction Factors, P. K. Rao, E. G. Astling, and F. J. Winninghoff (October 1965)
 - 35. Project Storm Cloud - An Aircraft - Satellite Case Study of an East Coast Cyclone, Part 1 - Descriptive Aspects, E. P. McClain and L. F. Whitney, Jr. (December 1965)
 - 36. Experimental Use of Satellite Pictures in Numerical Prediction, Part II, H. J. Brodrick, E. P. McClain and M. A. Ruzecki, (January 1966)